Sensorless Field Oriented Control with Embedded Power SoC

Z8F68474109

Scope and purpose of this document

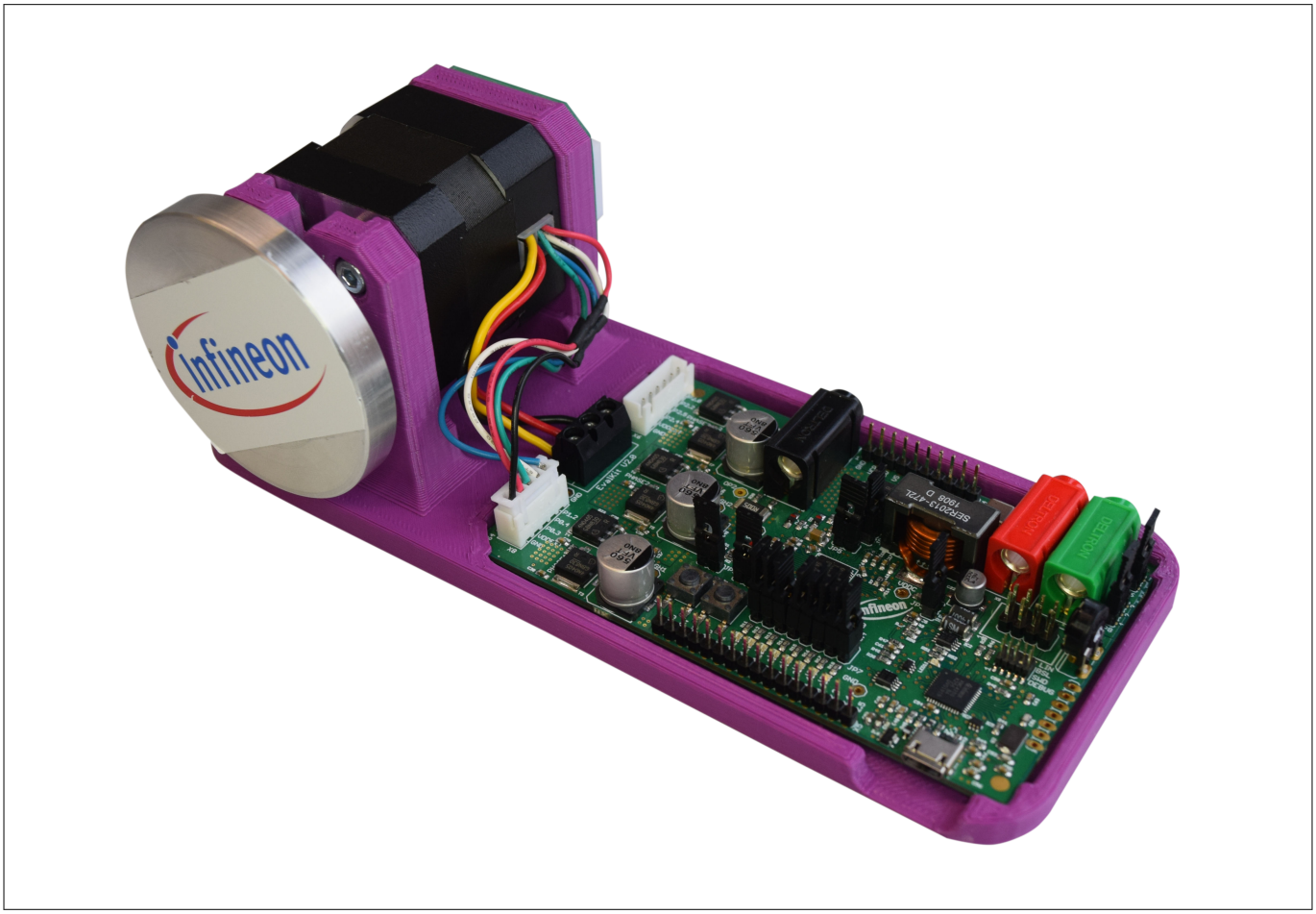

Figure 1

This document is meant to give the reader a basic introduction to field oriented control and how it can be implemented on the Infineon embedded Power SoC devices for low-to-mid power 3-phase motors in automotive applications. It is expected that the reader is familiar with the principles of motor control and its implementation on a microcontroller based system.

The full functionality and characteristics of the embedded power devices is specified in the respective datasheet and user's manual. Please refer to these documents for detailed description. The ***TLE9879 EvalKit*** has been used as hardware platform for the presented measurements, This EvalKit's schematic and PCB layout are the optimal starting point for developing new motor control ECUs. Similarly, the associated software project for the FOC implementation is meant as a demonstration platform.

Note: *The following information is given as a hint for the implementation of the system only and shall not be regarded as a description or warranty of a certain functionality, condition or quality of the referred devices or presented software example.*

Terms and abbreviations

Table 1 Terms used in this document

Abbreviation	Meaning
AC	Alternating Current
ADC	Analog to Digital Converter
BLDC	Brushless DC motor
BOM	Bill of Materials
CPU	Central Processing Unit
DC	Direct Current
ECU	Electronic Control Unit
BEMF	Back Electro Motive Force
EMC	Electromagnetic Compatibility
FOC	Field Oriented Control
MCU	Microcontroller
NVM	Non-volatile Memory
PMSM	Permanent Magnet Synchronous Motor
PWM	Pulse Width Modulation
SDK	Software Development Kit
SoC	System-on-Chip

Table of contents

Table of contents

1 Introduction

The Field Oriented Control (FOC) method described in this document is aimed at the growing market for cost-sensitive automotive drives, such as fans, pumps and geared motors. It is generally agreed that two main vectors have been driving the adoption of FOC-driven three phase motors in the automotive market: system cost and energy efficiency.

Sensors, indeed, require additional cost both for the sensing element and the required wiring harnesses and connectors. This may generate problems in manufacturing and act as a source of faults, reducing reliability.

The other major vector is the significant improvement of energy efficiency of a motor. FOC methodology allows for efficiency of up to 95%. This significantly reduces power consumption and improves motor dynamics, heat dissipation and noise. For example many fans and pumps applications required silent operation, in order to limit solid-borne sounds which eventually propagate in water or air pipes within the car cabin. Usually this leads to control techniques resulting in sinusoidal currents in the motor coils.

The Infineon Embedded Power SoC (system-on-chip) devices allow the implementation of 3-phase motor control ECUs optimized for both system size and cost. The SoC integrates the MCU and all necessary peripherals on a monolithic IC, with only the power stage's MOSFETs as additional external semiconductor devices. A major feature is the integrated bridge driver with its innovative gate driver which simplifies development and system optimization (e.g. improvement of EMC performance and adaptive capabilities to a wide range of different power stages characteristics).

2 Theory of Sensorless Field Oriented Control

This chapter is intended to give an overview about the theory of the sensorless FOC of permanent magnet synchronous motors (PMSM). The control scheme which has been implemented with the TLE987x is based on the theory described in this Chapter.

In these paragraphs the reader can find a summary about DC electrical motors and motor control, as well as a description of FOC theory. Details about the TLE987x implementation of these algorithms are described in Chapter ***Implementation of Sensorless FOC with the TLE9879 Embedded Power SoC***.

2.1 2-Phase (DC) Motor Basics

The 2-Phase motor, also known as DC motor, consists of a permanent magnet, which forms the stator structure, and a coil wrapped around the rotor. A mechanical commutator, the so called “brushes” mechanism, is needed in order to feed the current to the coils. This commutator will automatically switch the current orientation in order to allow for the right torque generation in all rotor positions.

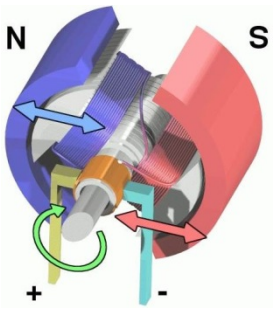

Figure 2 DC Motor

The 2-Phase Motor is controlled by regulating the voltage amplitude at the brushes while the resulting current is proportional to the torque of the motor. The speed of the motor depends on both the voltage and the torque.

The nominal speed (ω) and electric torque (T_e) are defined in the following equations:

$$\omega = \frac{u_a - i_a \times R_a}{c_E \times \psi_f} = \frac{u_a - i_a \times R_a}{k_E}$$

Equation 1

$$T_e = c_t \times \psi_f \times i_a = k_T \times i_a$$

Equation 2

Where:

ua is the voltage applied to the rotor coil

ia is the current flowing through the rotor coil

Ra is the rotor’s coil resistance

cE, ct are the motor constants (usually identical)

ψf is the magnetic field flux linked to the coil’s defined area

KE is the electrical constant of the motor

KT is the mechanical constant of the motor

The time constants of speed and current control are different by orders of magnitude, hence a control cascade structure for speed and current control can be utilized effectively.

2.1.1 2-Phase Motor Control: Open Loop Voltage Control

In an open loop voltage control, a reference voltage is input into the power stage, which will generate a given voltage at the motor. The mechanical load influences the speed and the current of the DC motor.

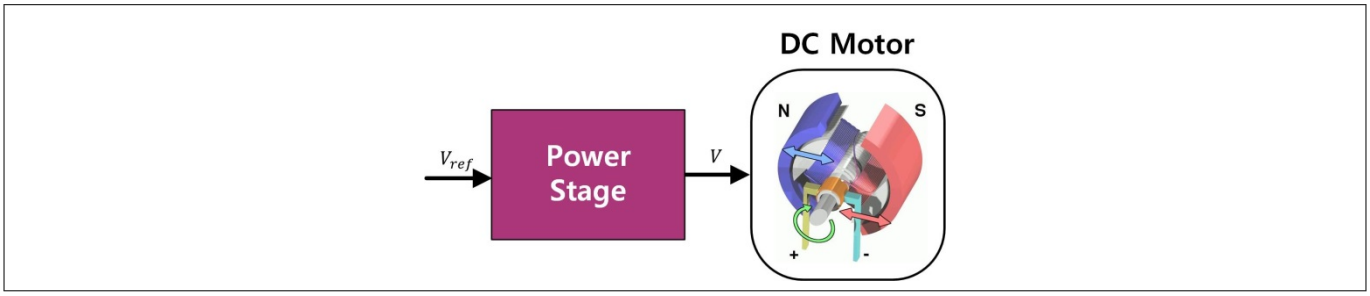

Figure 3 Open Loop Voltage Control

In steady state, the torque can be described by solving equation x and y which results in the following equation:

$$T_e = \frac{c_t \times \psi_f}{R_a} \times u_a - \frac{c_E \times c_t \times \psi_f^2}{R_a} \times \omega$$

Equation 3

2.1.2 2-Phase Motor Control: Closed Loop Torque Control

The torque control loop requires the measurement of the motor current with a current sensor; e.g. a shunt resistor. As seen in paragraph 2.1, in general the torque is proportional to the current .

$$T_e = k_T \times i_a$$

Equation 4

Thus, the torque reference can be set by giving an input current reference. The actual current, measured by the current sensor can be controlled with a PI controller in order to follow to the reference current. This will result in the regulation of the reference voltage (V_{ref}) for the power stage. Please see the following figure for details:

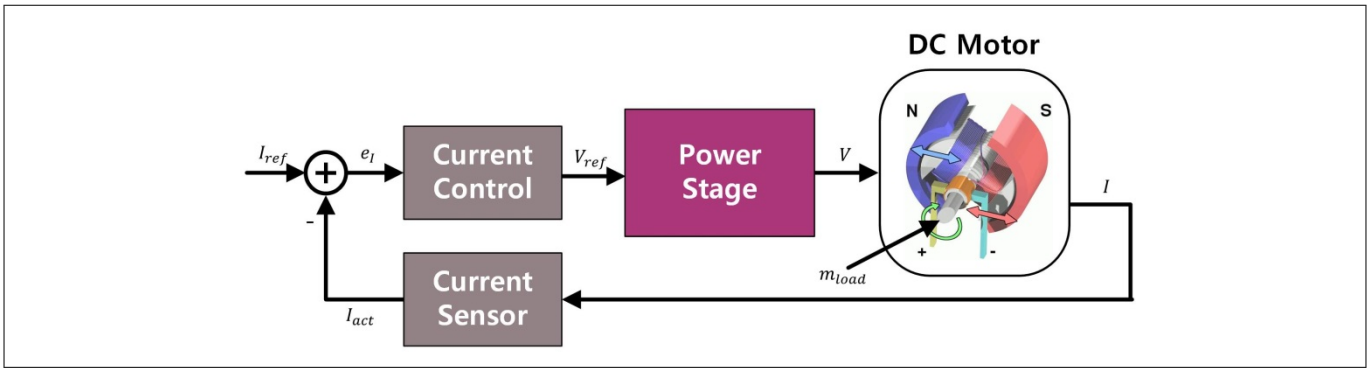

Figure 4 Closed Loop Torque Control

2.1.3 2-Phase Motor Control: Closed Loop Speed and Torque Control

As anticipated, a cascaded control structure can be used, because the speed change requirement is typically much slower than the one for the current, hence for the torque. The speed control requires a speed sensor, e.g. a tachometer, and the torque control requires a current sensor as seen in point 2.1.2. The output of the speed control is the reference current for the current control. Usually a PI controller is used both for speed and current control.

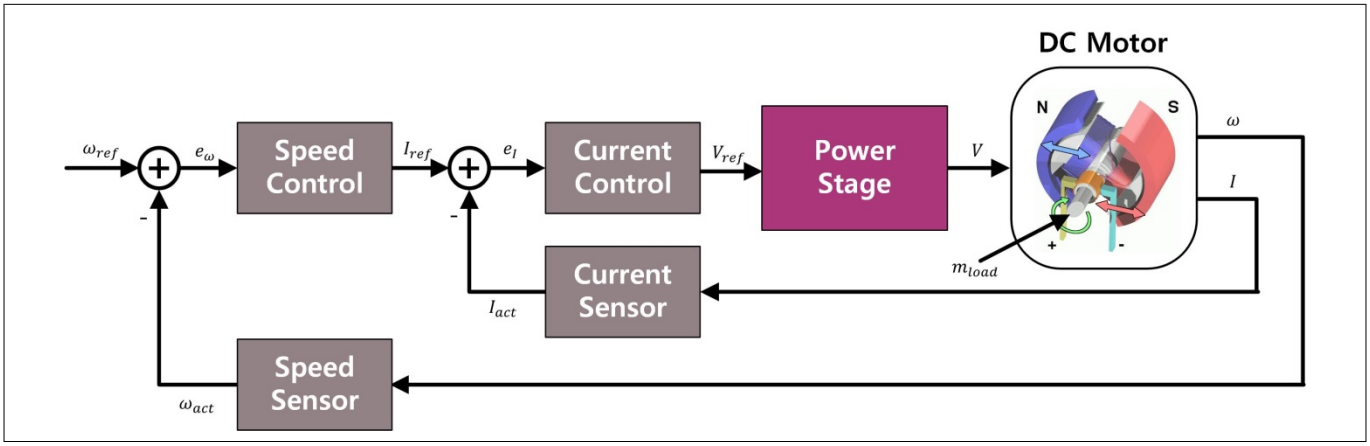

Figure 5 Cascaded Speed and Current Control

2.1.4 List of Equations

The electrical equations of the DC motor are also valid for the 3-phase motor. In the following, a set of equations is listed, which will be used later in this application note.

$$u_a = R_a\, i_a + L_a \frac{di_a}{dt} + e_a$$

Equation 5 **Voltage equation (for one phase)**

$$e_a = c_E\, \psi_f\, \omega = k_E\, \omega$$

Equation 6 **Induced voltage**

$$\phi = \int \omega dt$$

Equation 7 **Angle**

$$n = 60 \frac{\omega}{2\,\pi}$$

Equation 8 **Speed, in revolutions per minute (RPM)**

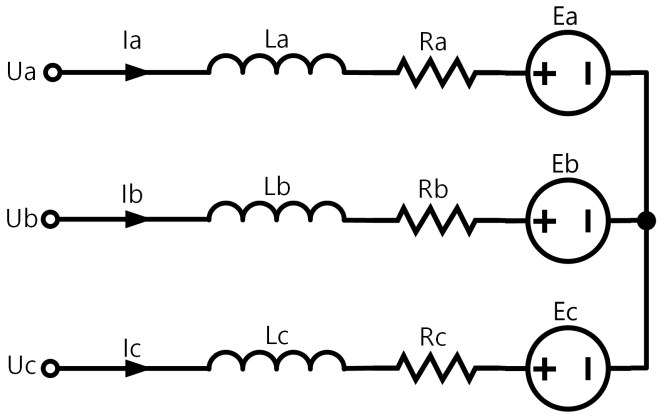

Figure 6 **BLDC motor equivalent circuit**

2.2 3-Phase Motor Basics

Most 3-phase PMSM motors for low to medium power automotive application are also called BLDC motors. As different terms are used in published literature, a short explanation and comparison amongst them will be given.

The term BLDC stands for brushless DC motor. This term may lead to confusion at first glance, considering that 3-phase motors, including BLDC motors, require AC currents to be able to turn. However, this term is meant to highlight the similarities between the two-phase (or DC) and three-phase BLDC electric motors. In fact, the BLDC construction is similar in a key aspect: the torque equation of the BLDC is analogous to the one of the brushed DC motor (see chapter ***2-Phase Motor Control: Closed Loop Torque Control***), as both are directly proportional to current.

However, contrarily to the DC brushed motor, the BLDC is built with electromagnetic coils in the stator and permanent magnets on the rotor – indeed it is often described as an “inside-out” DC motor. This construction solves several of the disadvantages of the DC motor by substituting the mechanical commutation operated by the brushed with electronic commutation served by a 3-phase bridge, also called inverter. Some of the typical advantages of the BLDC motor are:

- avoiding energy losses in the brushes
- saving brush maintainance costs
- improved reliability by not having mechanical brushes at risk of failure

The term PMSM emphasizes the construction of the motor with coils in the stator and permanent magnets in the rotor, as well as the fact that it rotates at a proportional speed to the coils alternating current’s frequency. Since these properties are shared by the BLDC motor, some publications consider a BLDC a subtype of PMSM motor.

In the industry, however, the terms BLDC & PMSM are often used in opposition to each other. The difference in this usage is in the construction of the stator windings. The term BLDC motor is used for those which have concentrated windings and surface mounted magnets while PMSM is used, more generally, when windings are sinusoidally distributed or magnets aren’t surface mounted. This difference in the construction affects the flux linkage between the magnet and the colis. This causes the back electro motive force (BEMF) voltage of the BLDC to have a trapezoidal form while the BEMF of the PMSM is sinusoidal.

2.3 Space Vector Modulation

In this section, the modulation of a three leg voltage inverter is described. This type of inverter is made of six MOSFETs or IGBTs which act as switches. The switches connected to the positive supply rail are called high-side switches (HSS) and the switches connected to the negative rail of the power supply are called low-side switches (LSS).

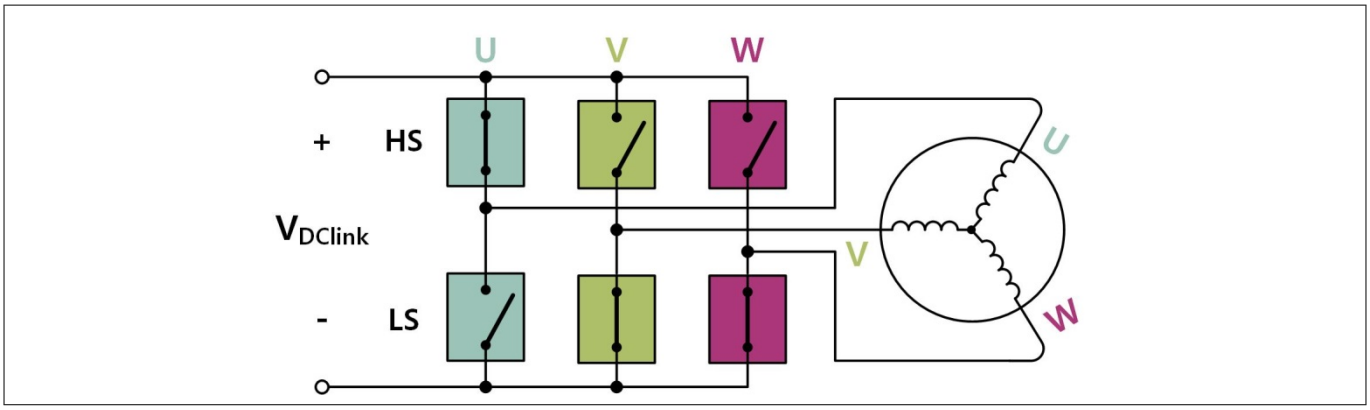

Figure 7 Three Leg Voltage Source Inverter

In the ***Figure 7*** a block diagram of a three leg voltage source inverter can be seen. If we exclude states in which the high and low switch of the same leg are turned on at the same time, as this would cause a short circuit, there are eight states possible, as shown in ***Figure 9***, each of them with different combinations of high and low side switches active. In each of these states, the three phases would cause three different magnetic fields, which can be visualized as vectors called magnetic dipoles. The combination of the effects of these fields can be visualized as a combined field, resulting in the sum of the vectors as shown in ***Figure 8*** in the form of complex numbers.

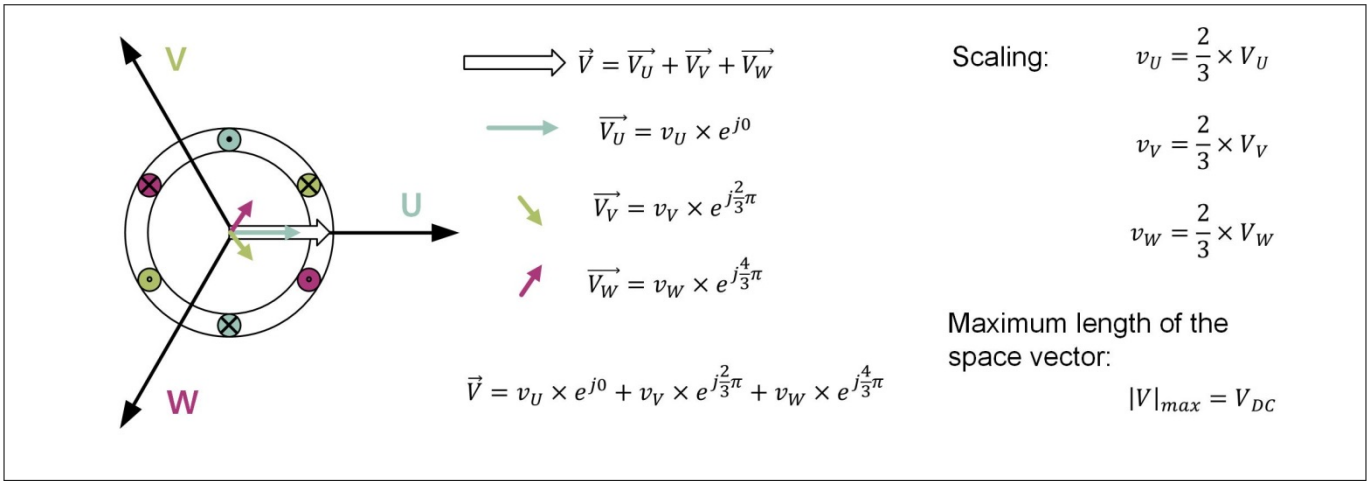

Figure 8 Space Vectors in Comples Numbers

Thus, the states themselves can be associated to a resulting magnetic field expressed as a vector in the space vector diagram of the coordinates U, V and W. There are two passive states leading to two null vectors, which do not cause a magnetic field, and six active states represented by non-null vectors. These active vectors divide the space vector diagram of a U-V-W system into six sectors, named A, B, C, D, E and F in ***Figure 9***.

State	U_{HS}	U_{LS}	V_{HS}	V_{LS}	W_{HS}	W_{LS}
000 (passive)	OFF	**ON**	OFF	**ON**	OFF	**ON**
100 (active)	**ON**	OFF	OFF	**ON**	OFF	**ON**
110 (active)	**ON**	OFF	**ON**	OFF	OFF	**ON**
010 (active)	OFF	**ON**	**ON**	OFF	OFF	**ON**
011 (active)	OFF	**ON**	**ON**	OFF	**ON**	OFF
001 (active)	OFF	**ON**	OFF	**ON**	**ON**	OFF
101 (active)	**ON**	OFF	OFF	**ON**	**ON**	OFF
111 (passive)	**ON**	OFF	**ON**	OFF	**ON**	OFF

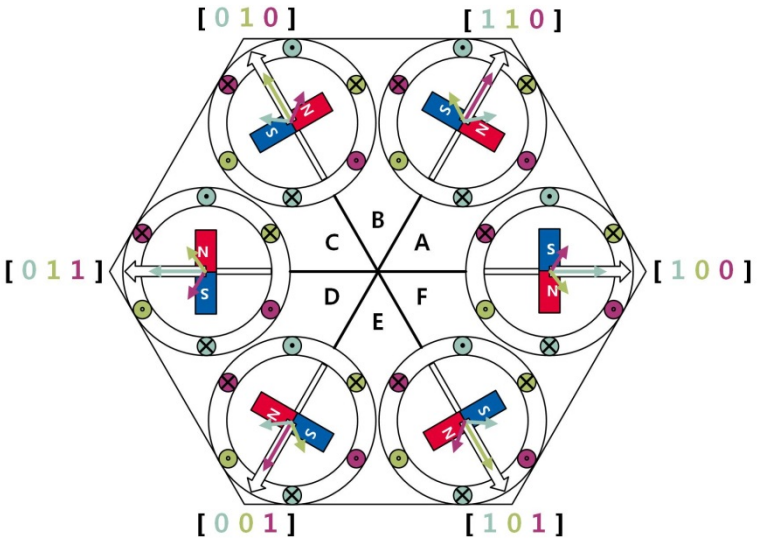

Figure 9 Space Vector Diagram of a U-V-W System

Despite the fact that the stator coils are fixed in their position, the magnetic dipole rotates dependent on the currents present in each phase. Considering any combination of voltages on the phases, their resulting magnetic stator field (flux) may be expressed by a reference vector V_{ref}. This one is defined by the following equation:

$$\overrightarrow{V_{ref}} = V_{ref} \times e^{j\varphi}$$

Equation 9

It is rotating in space with the speed (ω):

$$\omega = 2\pi \times f$$

Equation 10

This reference vector, if it is active, may be found in between any pair of the adjacent six active states, each of which is called a sector. Any position of the reference vector in a sector may be approximated by a linear combination of the two active vectors which define the sector (e.g. V_1 and V_2) and one zero vector (V_0). The attenuation factor needed for the two active vectors depends on the relative angle γ_{rel}, which is the absolute angle ϕ minus the angle of the first active vector in the sector (according to a clockwise rotation convention). This attenuation may be implemented physically by electrically changing the phase status significantly faster than V_{ref} changes. This means within a time Ts that we will call switching period, each one of the three active vectors must be applied for a certain duration so that the average vector voltage represents V_{ref} (see ***Figure 10***). This is the basis principle of pulse width modulation (PWM).

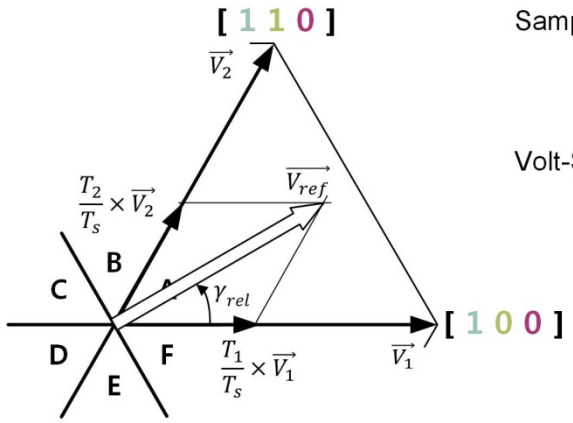

Sampling point:

$$T_s = T_1 + T_2 + T_0$$

Volt-Second balancing:

$$\overrightarrow{V_{ref}} \times T_s = \overrightarrow{V_1} \times T_1 + \overrightarrow{V_2} \times T_2 + \overrightarrow{V_0} \times T_0$$

Figure 10 Reference Vector Approximation

Taking into account the scaling of the reference vector and expressing the vector voltages as complex numbers, the following equations are valid for the PWM on-time (time during which the HSSs are on) of a space vector modulation:

$$T_1 = T_s \frac{V_{ref}}{V_{DC}} \sin\left(\frac{\pi}{3} - \gamma_{rel}\right)$$

Equation 11

$$T_2 = T_s \frac{V_{ref}}{V_{DC}} \sin(\gamma_{rel})$$

Equation 12

$$T_0 = T_s - T_1 - T_2$$

Equation 13

The design of the switching sequence depends on the application requirements. Usually the number of switchings is optimized in order to reduce switching losses.

The aim of the control is hence to calculate the duty cycle for each bridge phase that makes the V_{ref} rotate with the wanted electrical rotation.

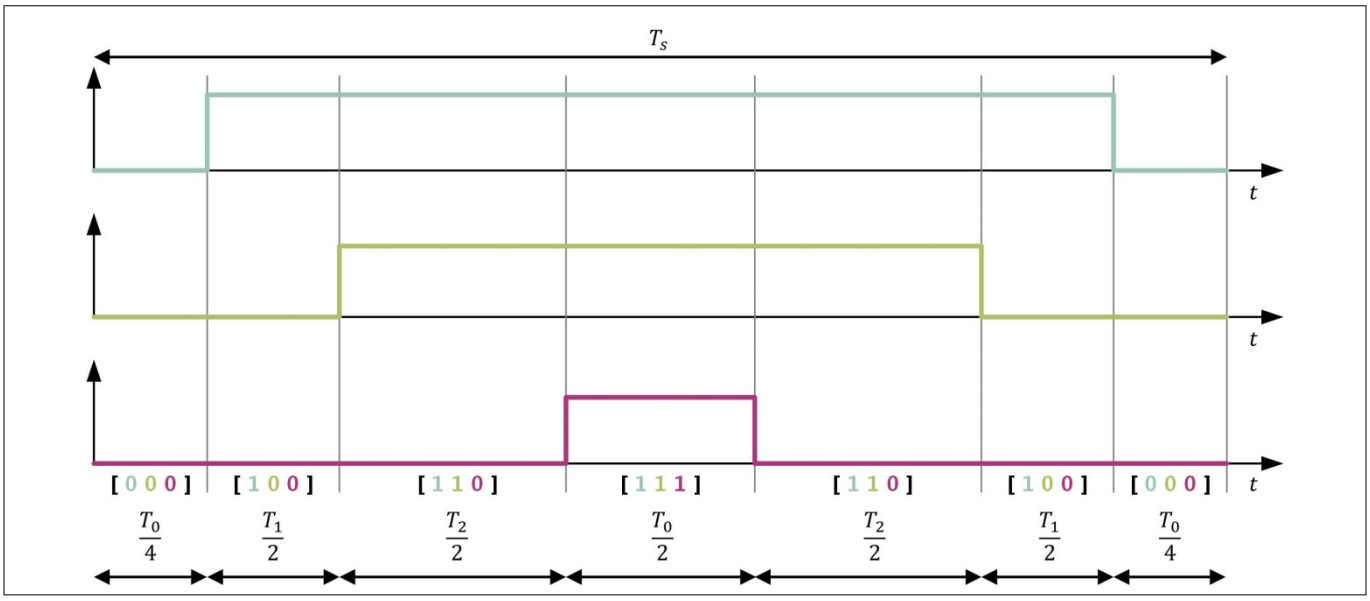

Figure 11 PWM Pattern of a Seven Segment Switching Sequence

An example of seven segment switching sequence during one PWM period Ts is shown in ***Figure 11***. The output voltage of each motor phase voltage vs neutral through the complete electrical rotation is shown in ***Figure 12***. The resulting voltages V_{UV}, V_{UW} and V_{VW} at the motor are sinusoidal.

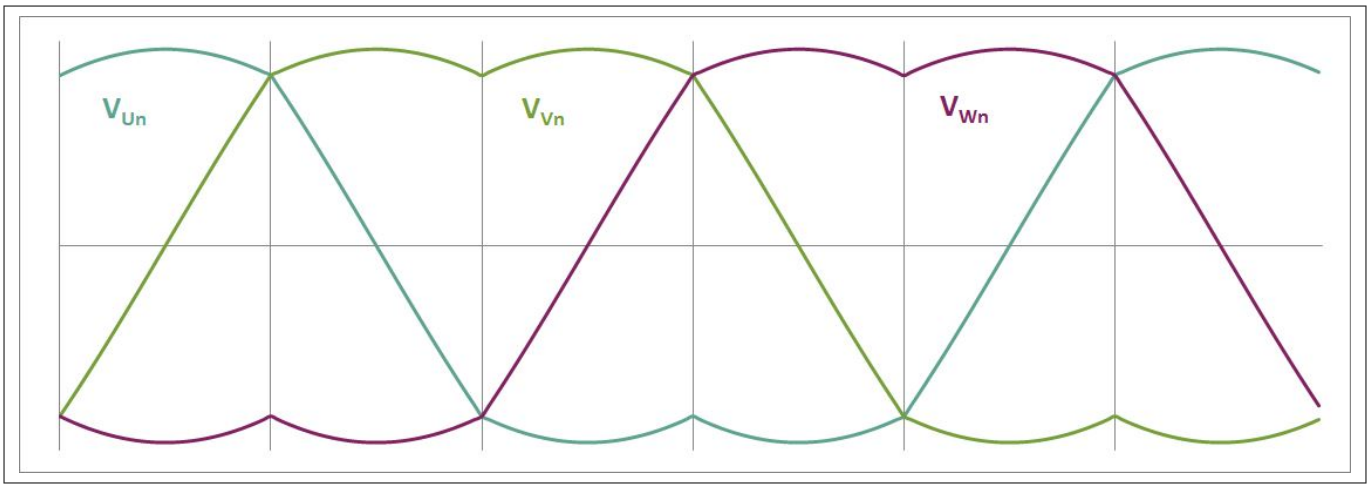

Figure 12 Output Voltage of Space Vector Modulation

2.4 Phase Current Measurement

For many motor control schemes, the phase currents are required as input values. A cost efficient method requires only one shunt in the DC-link. Two phase currents can be reconstructed from the DC-link current ($I_{DC-link}$) during one PWM period (T_s). The third phase current can be calculated by $I_U + I_V + I_W = 0$, but is redundant for the control. The current can be sampled with an ADC as shown in ***Figure 13***.

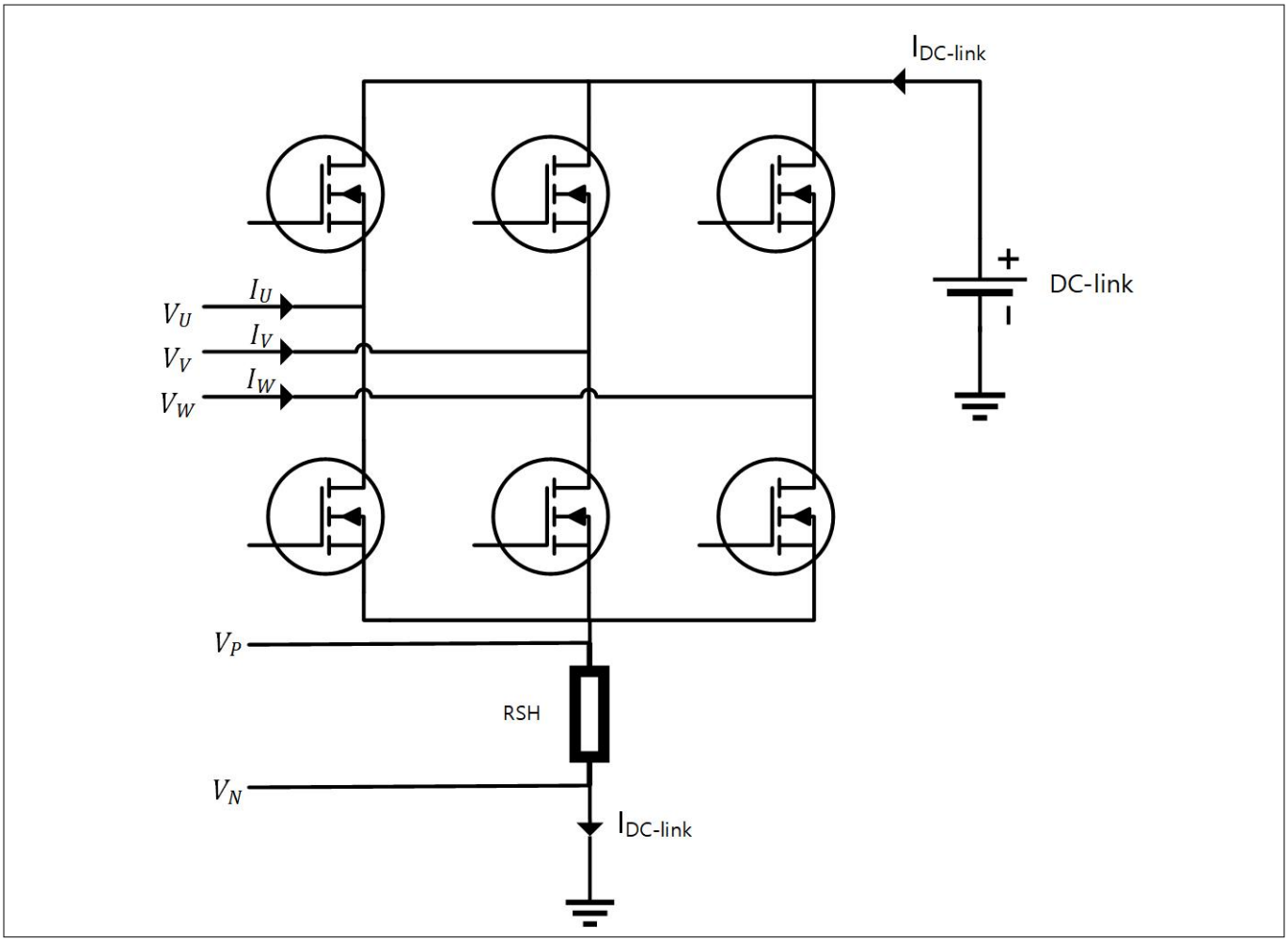

Figure 13 Simplified current sensing schematic

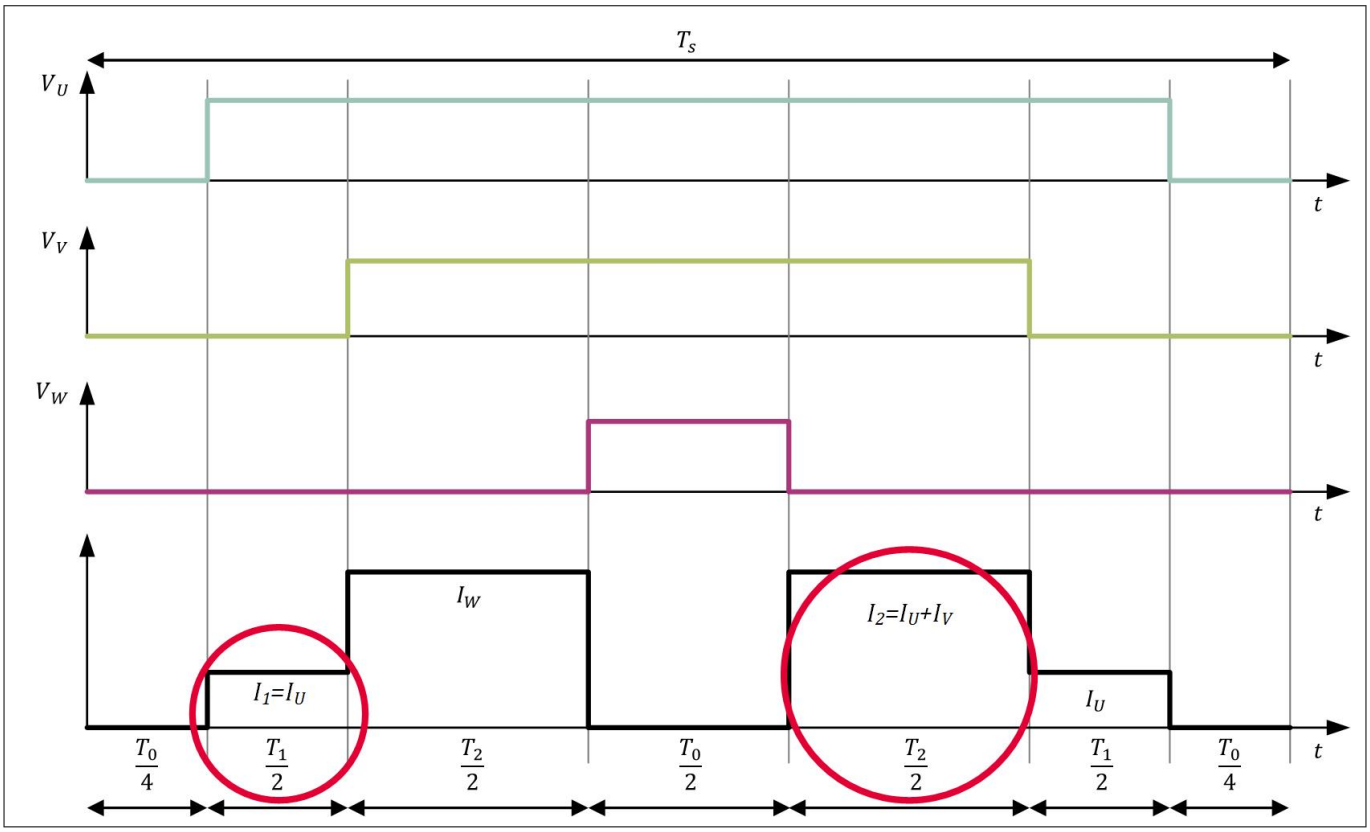

Figure 14 Phase Current Measurement within one PWM cycle in the SVM sector A.

In order to realize this method, the ADC trigger points must be adjusted according to the PWM pattern. Two different currents I_1 and I_2 can be measured at PWM time T_1 and T_2. Depending on the actual SVM sector, the measured currents I_1 and I_2 will have a different meaning. The following ***Table 2*** shows these combinations and the calculation for phase current I_A and I_B.

Table 2 Calculation for phase current IA and IB

Sector	A,0	B,1	C,2	D,3	E,4	F,5
I_1	I_U	I_V	I_V	I_WW	I_VW	I_U
I_2	I_U+I_V	I_U+I_V	I_V+I_W	I_V+I_W	I_U+I_W	I_U+I_W
$I_A = I_U$	I_1	I_2-I_1	$-I_2$	$-I_2$	I_2-I_1	I_1
$I_B = I_V$	I_2-I_1	I_1	I_1	I_2-I_1	$-I_2$	$-I_2$

2.4.1 Limitations of Phase Current Reconstruction

When T_1 or T_2 equals 0, only one phase current can be reconstructed. To avoid this situation, the PWM-times T_1 and T_2 have to be limited to a minimum value. This causes a ripple in the phase voltage and the phase current as well. ***Figure 15*** shows the output voltage and phase voltage of a T_1-T_2 -limited space vector modulation.

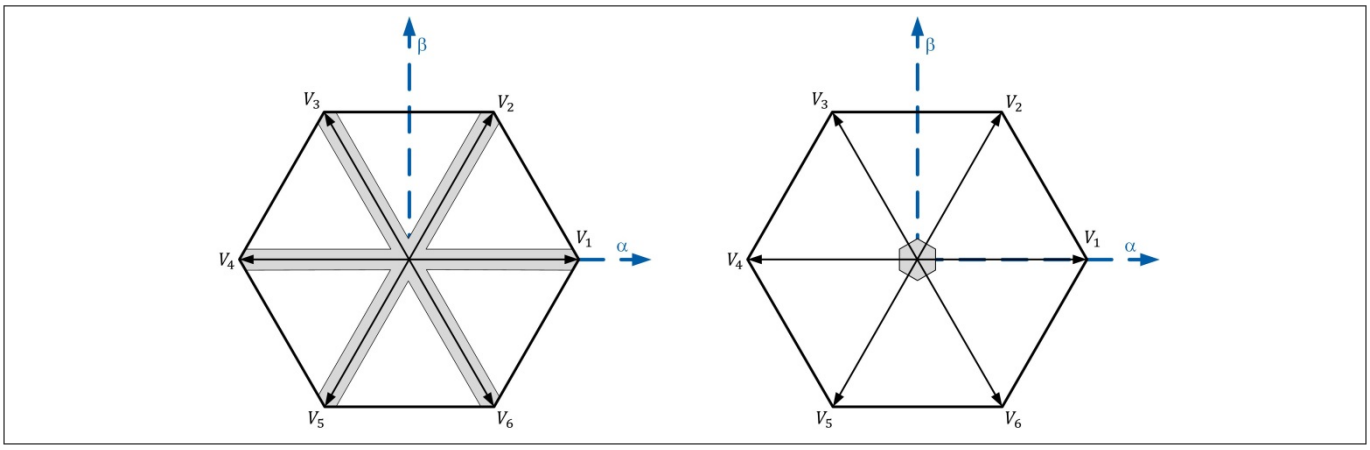

Figure 15 Space vector diagram with limitations caused by low duty cycles

Although the output signal is slightly distorted, the most cost efficient method of phase current measuring is the reconstruction from the DC_{link} current via a single shunt. A very fast ADC is required to optimize the system performance. A direct trigger from the PWM unit to the ADC reduces CPU load significantly.

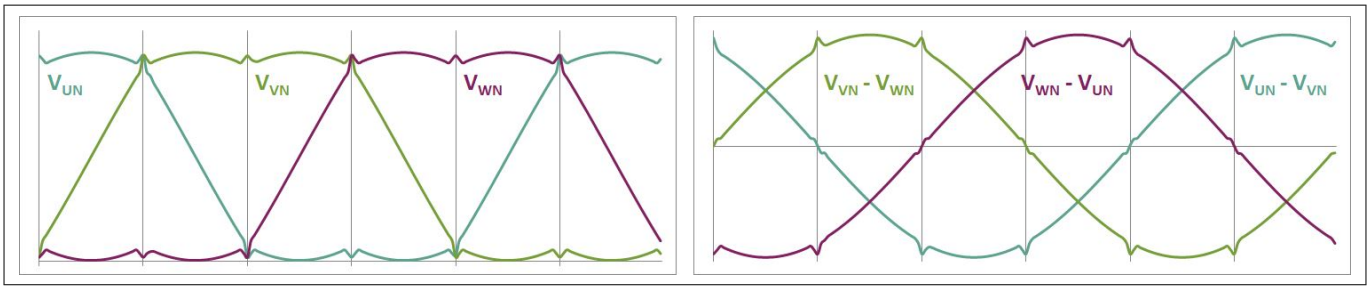

Figure 16 Distortion in Output and Motor Voltage

2.5 FOC Calculations

FOC is a method which generates a three phase sinusoidal modulation, which can easily be controlled in frequency and amplitude in order to minimize the currents and therefore maximize the efficiency. The essential idea is the transformation of three phase sampled current signals into two rotor-fixed signals and vice versa. In the rotor-fixed reference frame, the currents can be treated as stationary values and are easy to control. Using the inverse vector rotation the controller generated reference voltages can be returned to a rotating vector in the stator reference frame.

2.5.1 Stationary and Rotating Reference Frames

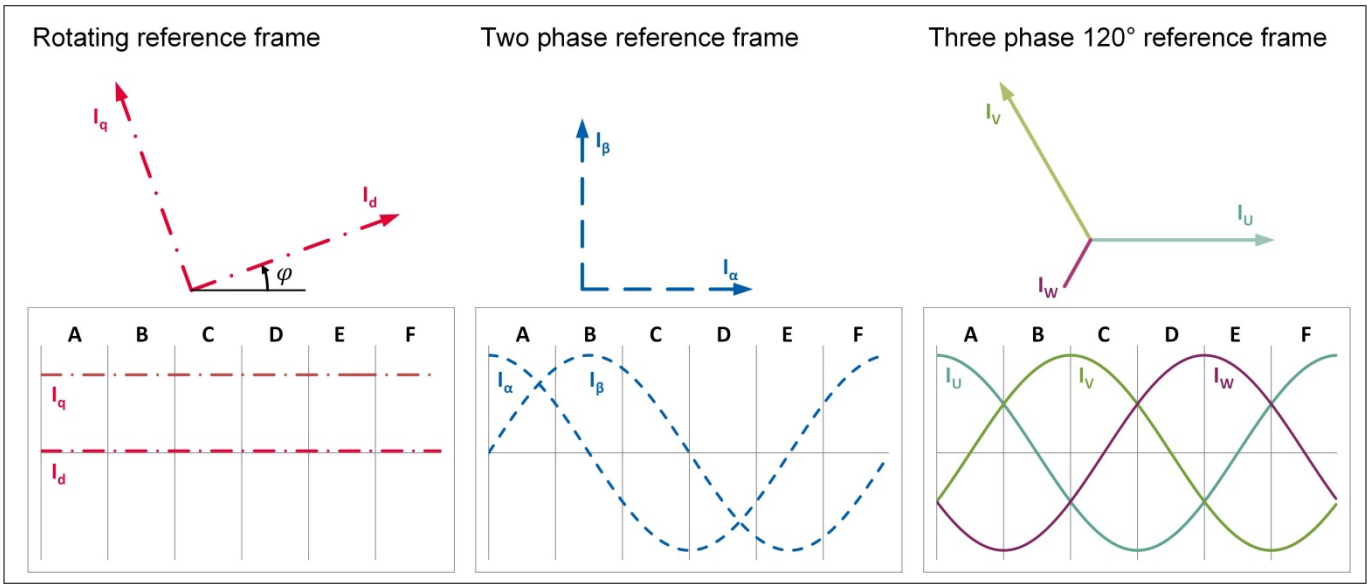

Figure 17 Stationary and Rotating Reference Frames

The transformation from the three phase system to the two phase system is called the Clarke transform, whereas the one from stationary to rotating two-phase system is called the Park transform. These transformations are expressed by the following equations:

Clarke Transform

$$i_\alpha = i_U$$

Equation 14

$$i_\beta = \frac{1}{\sqrt{3}}(i_U + 2i_V)$$

Equation 15

$$i_U + i_V + i_W = 0$$

Equation 16

Park Transform

$$i_d = i_\alpha \cos(\varphi) + i_\beta \sin(\varphi)$$

Equation 17

$$i_q = -i_\alpha \sin(\varphi) + i_\beta \cos(\varphi)$$

Equation 18

Inverse Park Transform

$$i_\alpha = i_d \cos(\varphi) - i_q \sin(\varphi)$$

Equation 19

$$i_\beta = -i_d \sin(\varphi) + i_q \cos(\varphi)$$

Equation 20

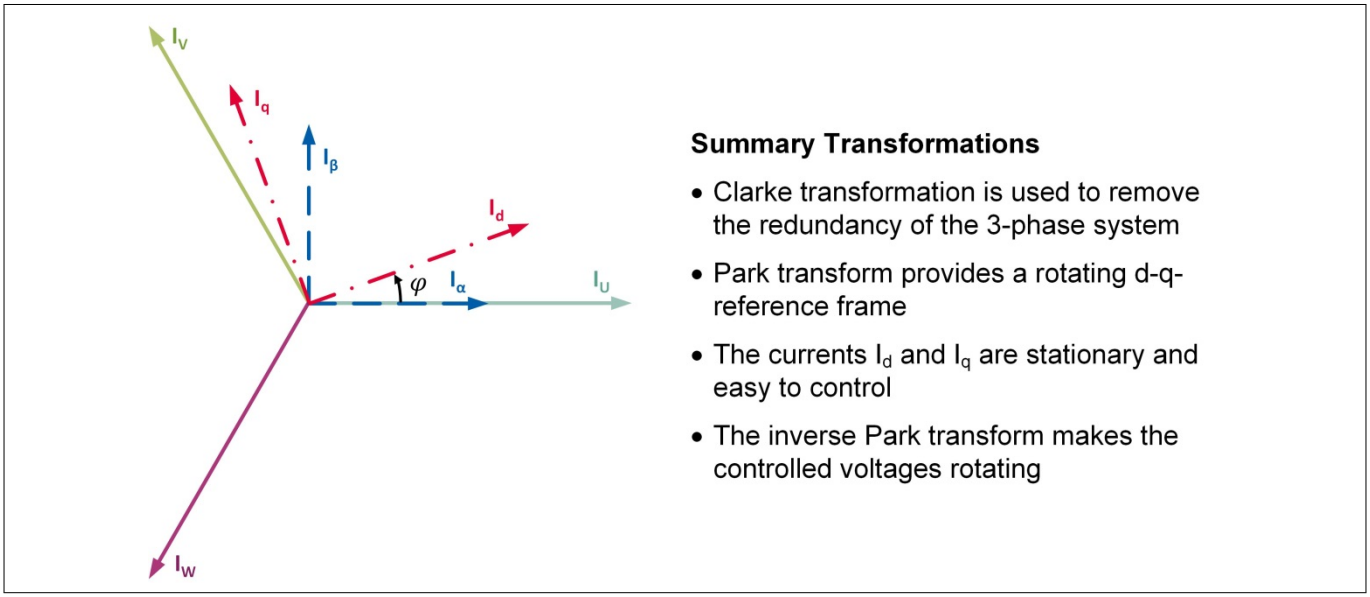

Figure 18 Summary of Transformations

2.5.2 Sensorless FOC

Sensorless operation offers the great advantage of saving the costs for an encoder or other position sensor. In order to achieve this, the motor's rotor flux is utilized to calculate the rotation angle and thus estimate rotor position. The rotor flux itself is calculated in the flux estimator, which extracts the back EMF from the applied phase voltage by subtracting all voltage drops not associated with the back EMF. The rotor flux is then found by integration of the estimated back-EMF. Sensorless algorithms are less reliable when the applied phase voltage or measured current is inexact, such as for low speed operation.

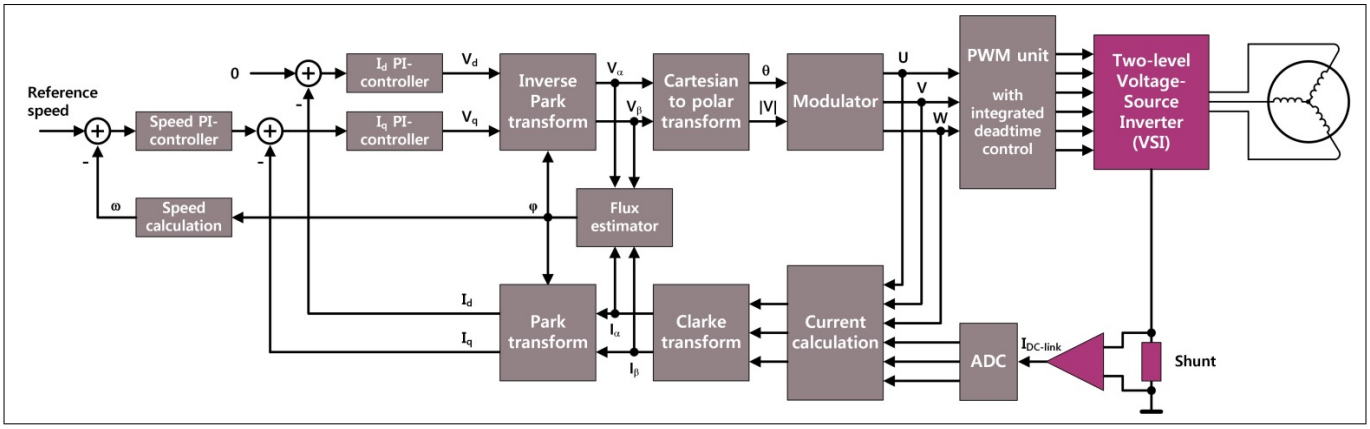

Figure 19 Block Diagram of Sensorless Field Oriented Control

Figure 19 shows the block diagram of the sensorless FOC algorithm. In this example, the flux estimator's input signals are taken from the orthogonal two phase stator system with the index α and β. The output signal represents the rotor angle.

The motor signals in the two phase stator system (α-β-system) are equivalent to the three phase system. As a result, an ideal two phase motor can be assumed in the α-β-system. Then there are only two equations to calculate. The ***Figure 20*** shows the voltage equations of the motor in the α-β-system.

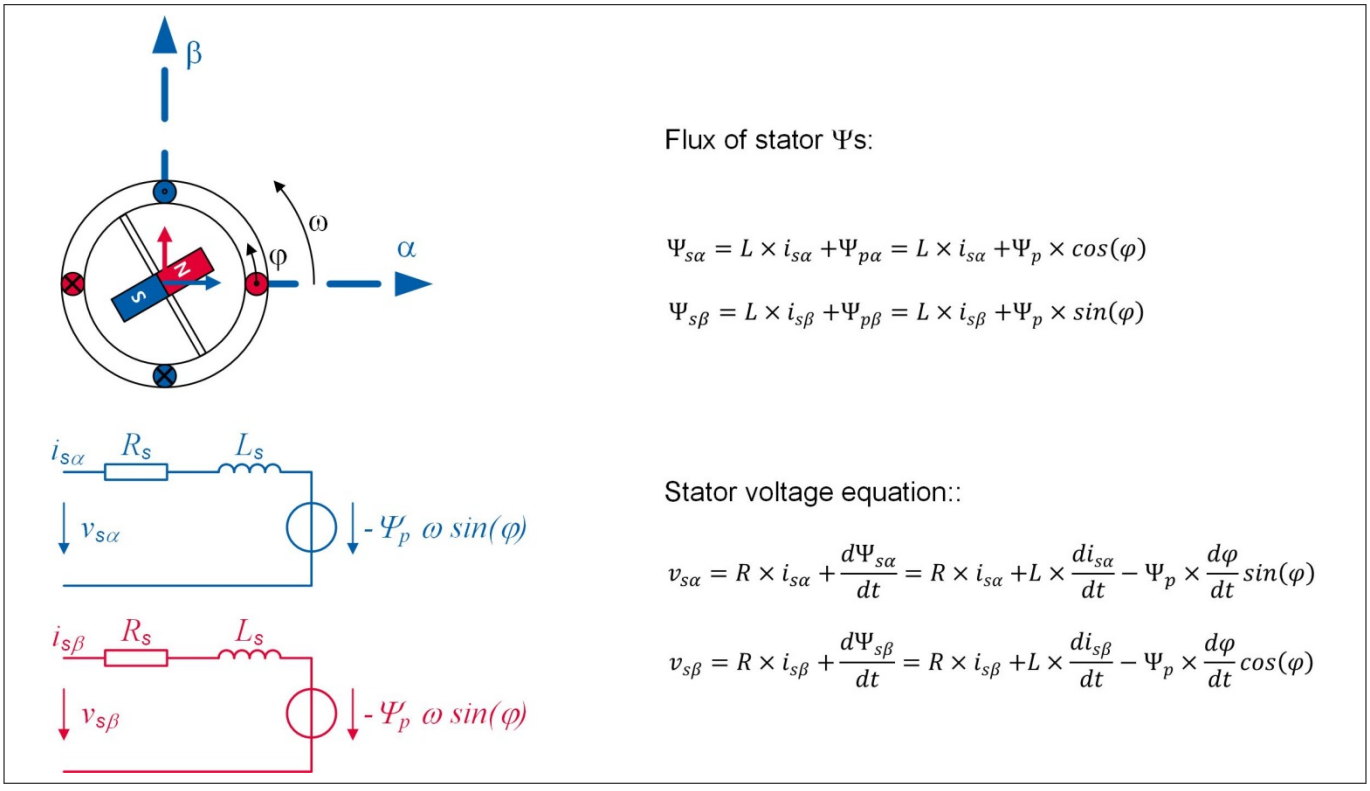

Figure 20 Voltage Equations of Ideal 2-phase Motor

The flux of the stator ($\Psi_{s\alpha}$ and $\Psi_{s\beta}$) contain the mutual inductance L × $\vec{i_s}$ and the flux of the rotor $\overrightarrow{\Psi_p}$ generated by permanent magnet.

The stator voltage equations ($v_{s\alpha}$ and $v_{s\beta}$) contains the resistance of the coil R × $\vec{i_s}$ and the derivative of the flux of the stator (Faraday's Law).
Integrating the voltage equations, we calculate the stator flux as follows:

$$\Psi_{s\alpha} = \int v_{s\alpha} - R\, i_{s\alpha}\, dt$$

Equation 21

$$\Psi_{s\beta} = \int v_{s\beta} - R\, i_{s\beta}\, dt$$

Equation 22

The flux of the rotor and hereby the orientation (angle ϕ) of the permanent magnet of the rotor is calculated by insertion:

$$\Psi_{p\alpha} = \Psi_{s\alpha} - L\, i_{s\alpha} = \int v_{s\alpha} - R\, i_{s\alpha}\, dt - L\, i_{s\alpha}$$

Equation 23

$$\Psi_{p\beta} = \Psi_{s\beta} - L\, i_{s\beta} = \int v_{s\beta} - R\, i_{s\beta}\, dt - L\, i_{s\beta}$$

Equation 24

$$\phi = \operatorname{atan}\left(\frac{\Psi_{p\beta}}{\Psi_{p\alpha}}\right)$$

Equation 25

The position of the rotor can be calculated by knowing the resistance R and inductance L of the motor. The stator voltage v_s is derived from the algorithm, and the current i_s needs to be measured in real-time.

3 Implementation of Sensorless FOC with the TLE9879 Embedded Power SoC

This chapter describes the implementation of a sensorless Field Oriented Control using the Infineon TLE9879 SoC. The TLE9879 integrates an ARM Cortex M3 32-bit microcontroller, digital peripherals, NVM memory and analog power peripherals in a 7x7mm 48-pin VQFN package. Together with an external power stage (MOSFET B6 bridge) the complete motor controller ECU can be realized in a very small footprint.

The 3 PWM units, several timers and very fast and powerful ADC make the TLE9879 a perfect fit for a variety of cost optimized motor control applications.

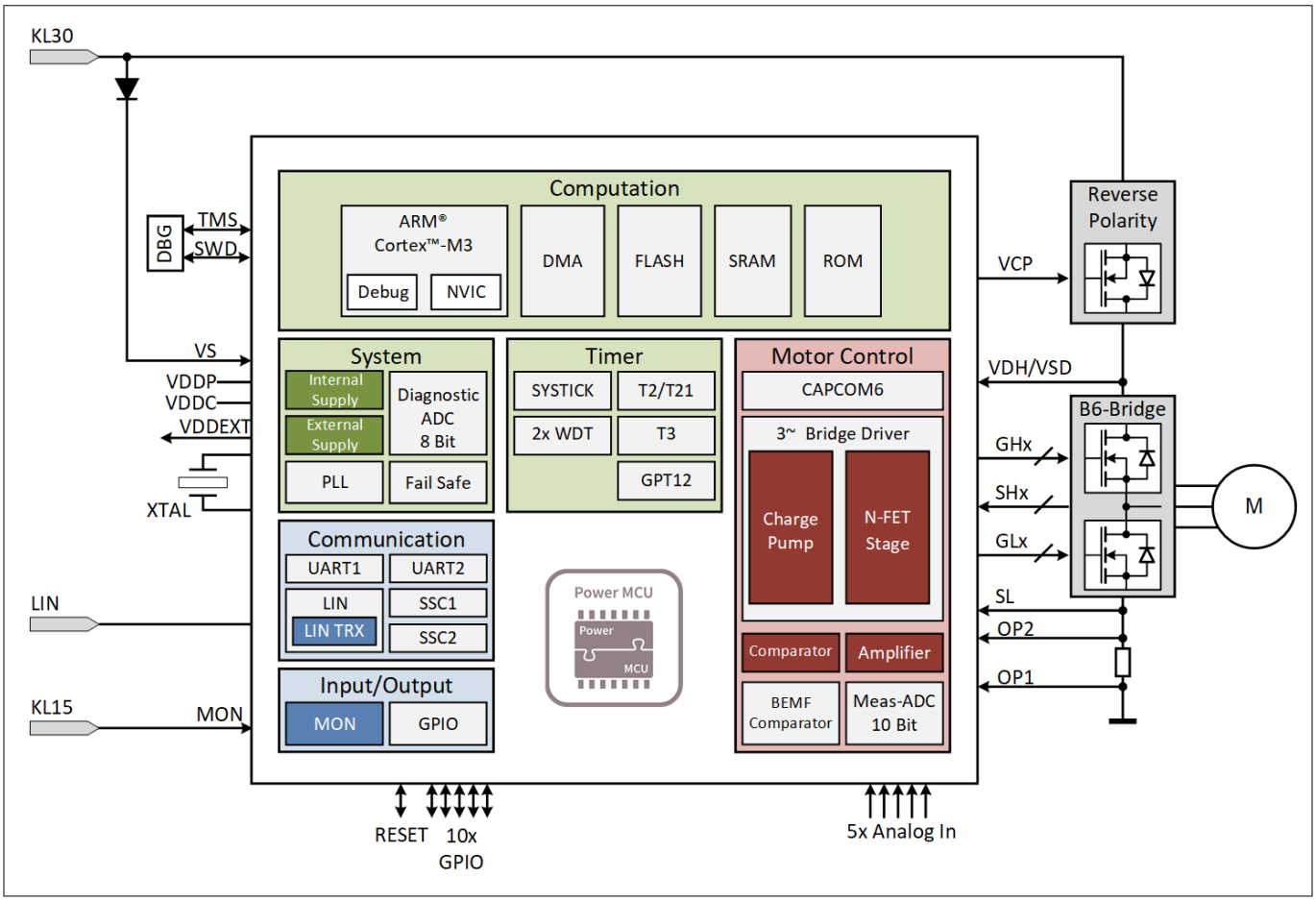

Figure 21 Block diagram of TLE9879

3.1 System overview

In typical applications for the TLE9879 SOC, the BLDC-Motor and the control ECU are mounted close to to each other (***Figure 21***). The control ECU typically contains the TLE9879, next to six MOSFETs for the 3-phase bridge, one MOSFET for reverse battery protection, and several passive components for protection, diagnosis and filtering.

3.2 Hardware components of TLE9879

This chapter will explain the usage of the key hardware modules of TLE9879 for Sensorless FOC applications.

3.2.1 ADC

The ADC module is used to convert the current measurement from the shunt resistance at the DC-Link to a digital value that can be used in the software. The measurement is performed twice during each PWM cycle, at points where different phases are active, relying on the software's knowledge of the implemented phase modulation pattern. These two measurements allow for the calculation of two phases, whereas the third is calculated by the equation $i_U+i_V+i_W=0$. A critical aspect for the measurement is to complete it before the PWM phase changes shifting to the next sector. This is achieved by starting the ADC measurement right after the voltage ringing caused by the last PWM switching across the shunt resistor has subsided and with enough time left to finish the measurement before the time of the measurement vector is over. Usually a good starting point is right in the middle of the measurement vector.

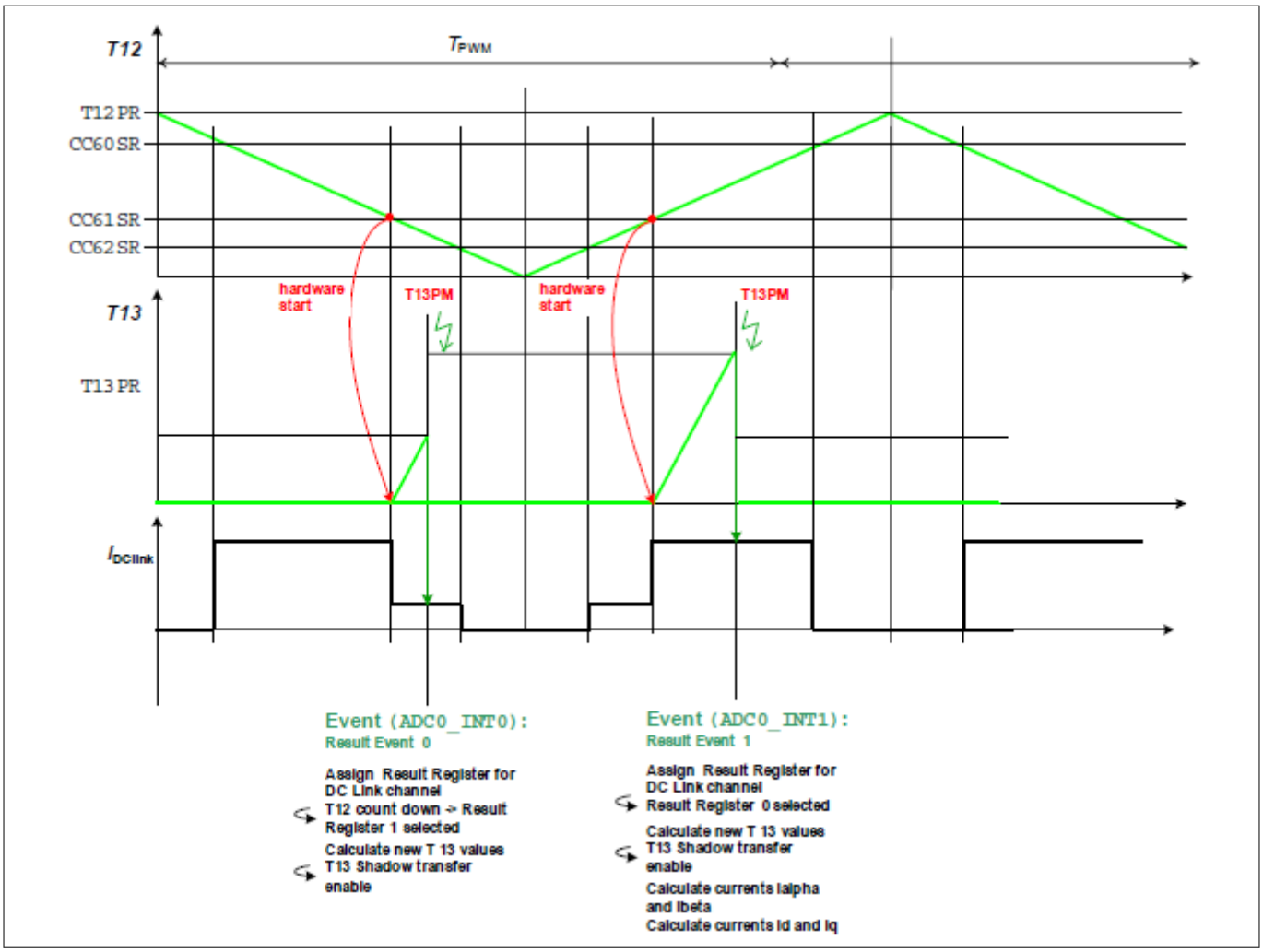

Figure 22 ADC Measurement

3.2.2 GPT12E

In the example, the GTP1 timer is set up so that each step is 100ns, counting up to 1.8311ms. This is the timing used by the speed pi controller in FOC.

3.2.3 CCU6

The CCU6 timer unit has beed designed to be able to generate the PWM signal by using both timers T12 and T13. T12 is used to generate the signals for the Space Vector Modulation (SVM), which is why it has three different compare values set on each single period. The timer's period is setup according to the PWM frequency, whereas the three compare values define the ON-time for the three phases. T13 is used in combination with T12 timing to generate the trigger events for the ADC. T13 runs in single shot mode and starts automatically on one defined compare match of one of the 3 compare channels. The generated trigger starts the conversion of the ADC1 channel which generates an interrupt after the channel is converted.

Additionally, the CCU6 can automatically add a deadtime. Depending on the MOSFET type used in the MOSFET half-bridges, the switch-on and switch-off times will change. In the worst case, the switch-on time is smaller than the time for switch-off and a short circuit in the inverter leg might occur. In order to guarantee safety of the motor bridge, the capture / compare unit contains a programmable Dead-Time Generation Block which can automatically add a delay between the switchoff on one MOSFET and the switch on of its compliment.

Please observe ***Figure 23*** below.

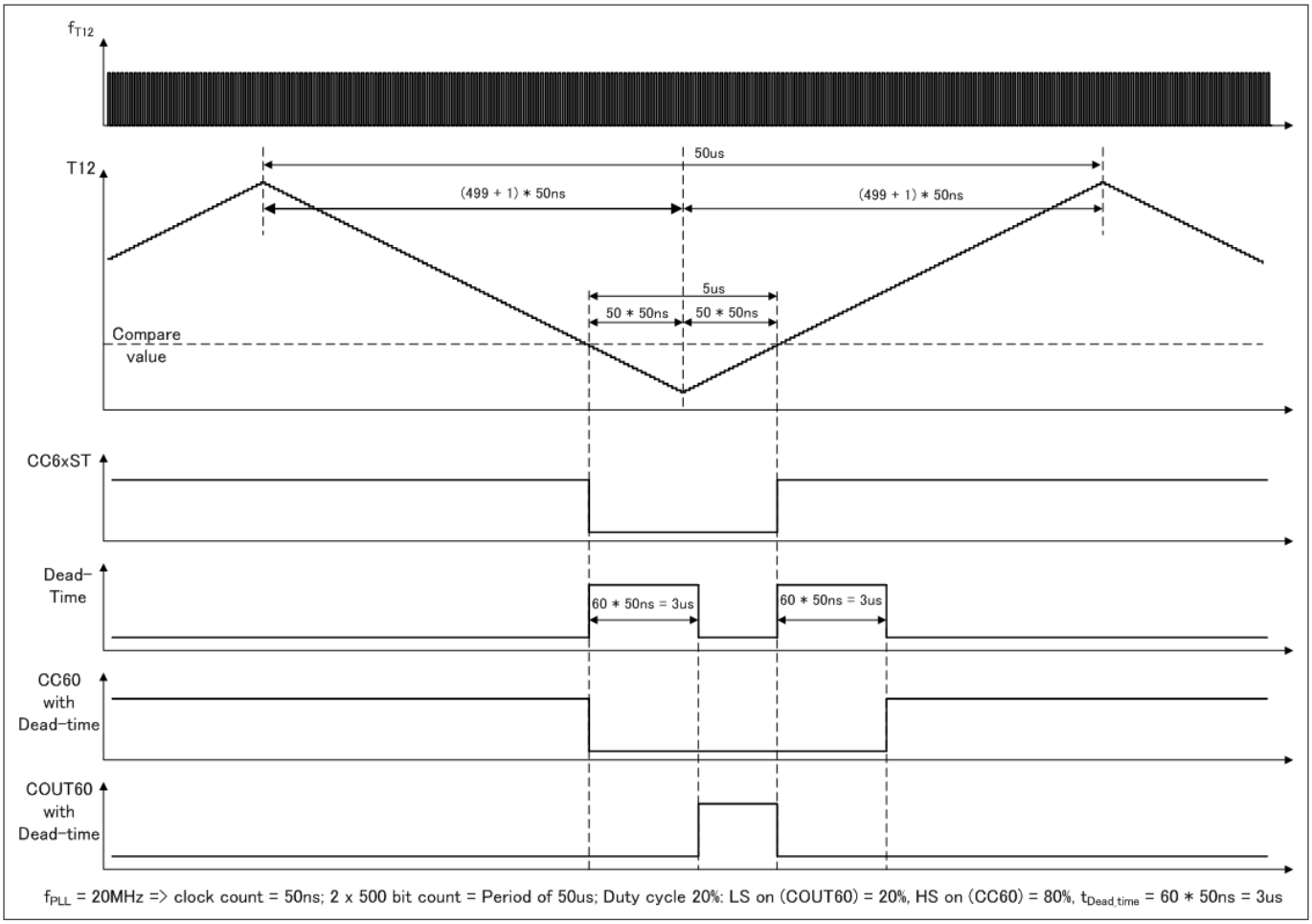

Figure 23 PWM gate signals with dead-times (center-aligned mode)

3.2.4 BDRV

The MOSFET Driver is intended to drive external normal level MOSFETs built in a Bridge configuration. In our case, the driver will deliver the physical implementation of the CCU6 signals.

The MOSFET driver is designed to drive N-MOSFETs due to them being standard in the industry. For this, the MOSFET driver needs to supply voltages over the supply voltage, which is typically 12V for the TLE9879. This is achieved through a two stage Charge Pump. The use of the charge pump enables a duty cycle range from 0 - 100%.

The regulated output voltage is typically V_S + 14V (V_S is typically the DC link voltage), but can be set to V_S + 9V if necessary. The charge pump output V_{CP} is monitored via an undervoltage comparator. If undervoltage is detected, the pumping is stopped and the drivers will be switched off.

3.2.5 Shunt Resistor & CSA

As discussed in the chapter 2, the key measured variable in Sensorless FOC is the DC-link current across the Shunt resistor. The TLE9879 example configuration uses a single shunt resistor, enabling a more cost-optimized solution for most low- to-mid power loads in a car, which do not require high dynamic capabilities.

The resulting voltage is then measured by ADC1 via an internal current sense amplifier, an external anti-aliasing low-pass filter (AAF) and a single shunt resistor as shown in ***Figure 24***

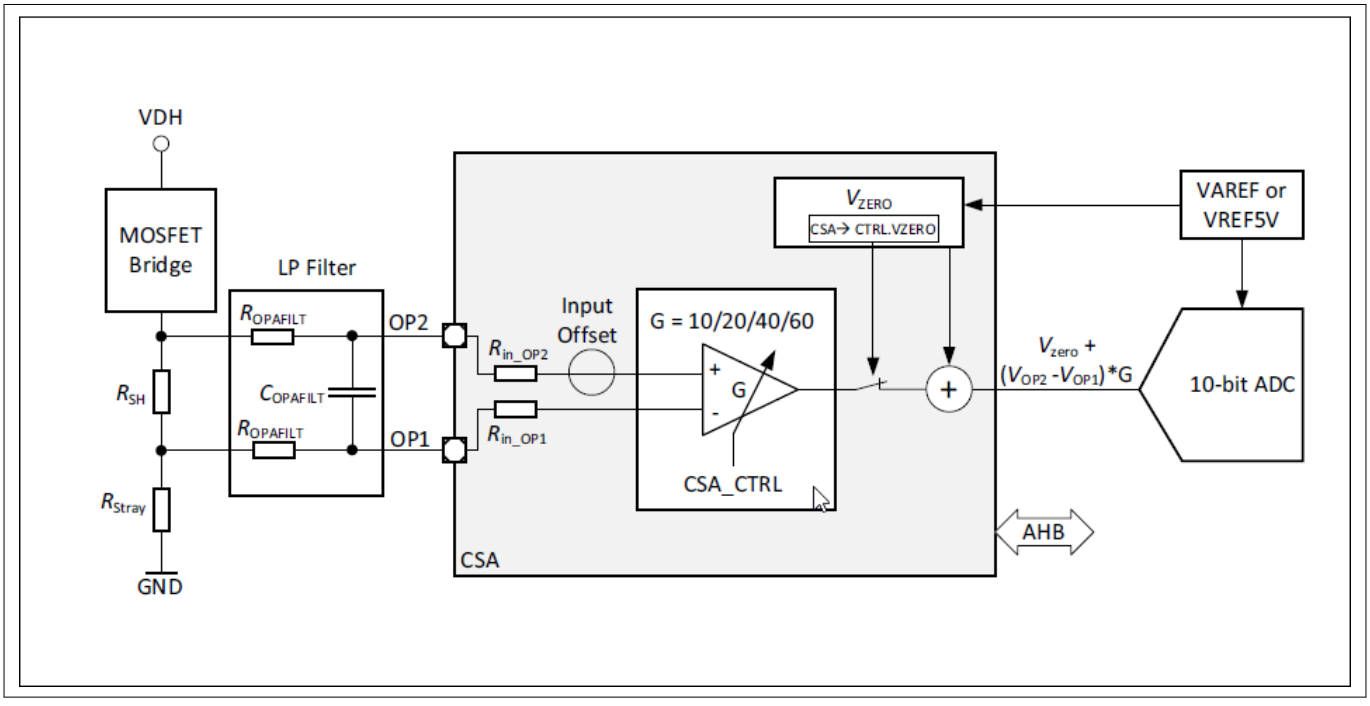

Figure 24 Motor current measurement

For this measurement, the key elements to be considered are the following:

- In the TLE987X SOC the ADC input voltage should not be higher than 5V because of the reference voltage. It means the voltage between shunt (VP – VN) should be less than 5V /G_{TOTAL}. If not, the ADC input stage will be saturated.
- The maximum allowed power dissipation of the shunt resistor should be higher than $(I_{MOT,max})^2 * R_{SH}$

The recommended value for the low-pass filter resistors R_{LP} is application specific. Please see our recommendations in the User Manual for a starting point. The filter should be designed to only filter out high frequency noise transients, and should influence the measured currents as little as possible.

4 Software Block Diagram

Figure 25 is a schematic software block diagram of the sensorless FOC example algorithm provided by Infineon for the TLE987X. It shows the major software components and focuses on their basic roles & connections. The main elements, starting from the current measurement on the right side, are a single shunt-based phase current measurement and reconstruction, a Clark transform that converts three-phase to two-phase, a Park transform that converts a rotating magnetic field into a fixed field, a cartesian transformation for angle position, a Flux Estimator to estimate the flux & rotor position, PLL to estimate and smoothen the angle position in the next PWM cycle, three PI Controllers to control velocity and the two fixed currents, a polar transformation for angle & amplitude to be input into to SVM, and the SVM to modulate the space vector in complex space into physical outputs.

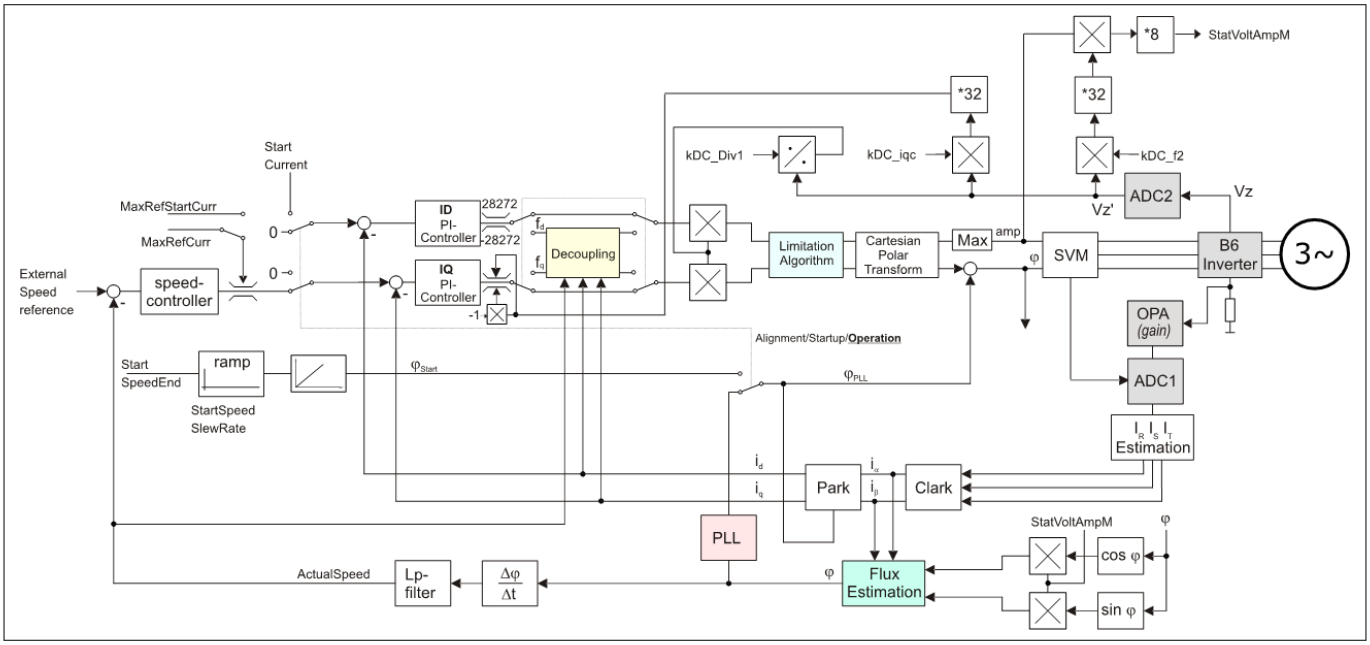

Figure 25 Software Block Diagram

A key feature of this software that can also be seen in this software block diagram is the existence of two different modes in the software – open and closed loop mode. As discussed in the theory section, one key weakness of sensorless software methods is that they rely on the BEMF, which is proportional to speed. Because of this, the Infineon example software includes a switch: it starts in open loop using a ramp angle for its modulation and after a configurable time, it switches to the closed loop and uses the estimated angle from the PLL.

4.1 Phase current measurement and reconstruction

The phase current detection is based on a single shunt and obtains the currents with two samples in one PWM period. The generation of the phases is based on comparison values at the Timer12 which operates in Center Aligned Mode. During this process, two shunt current measurements take place as shown in the following ***Figure 26***.

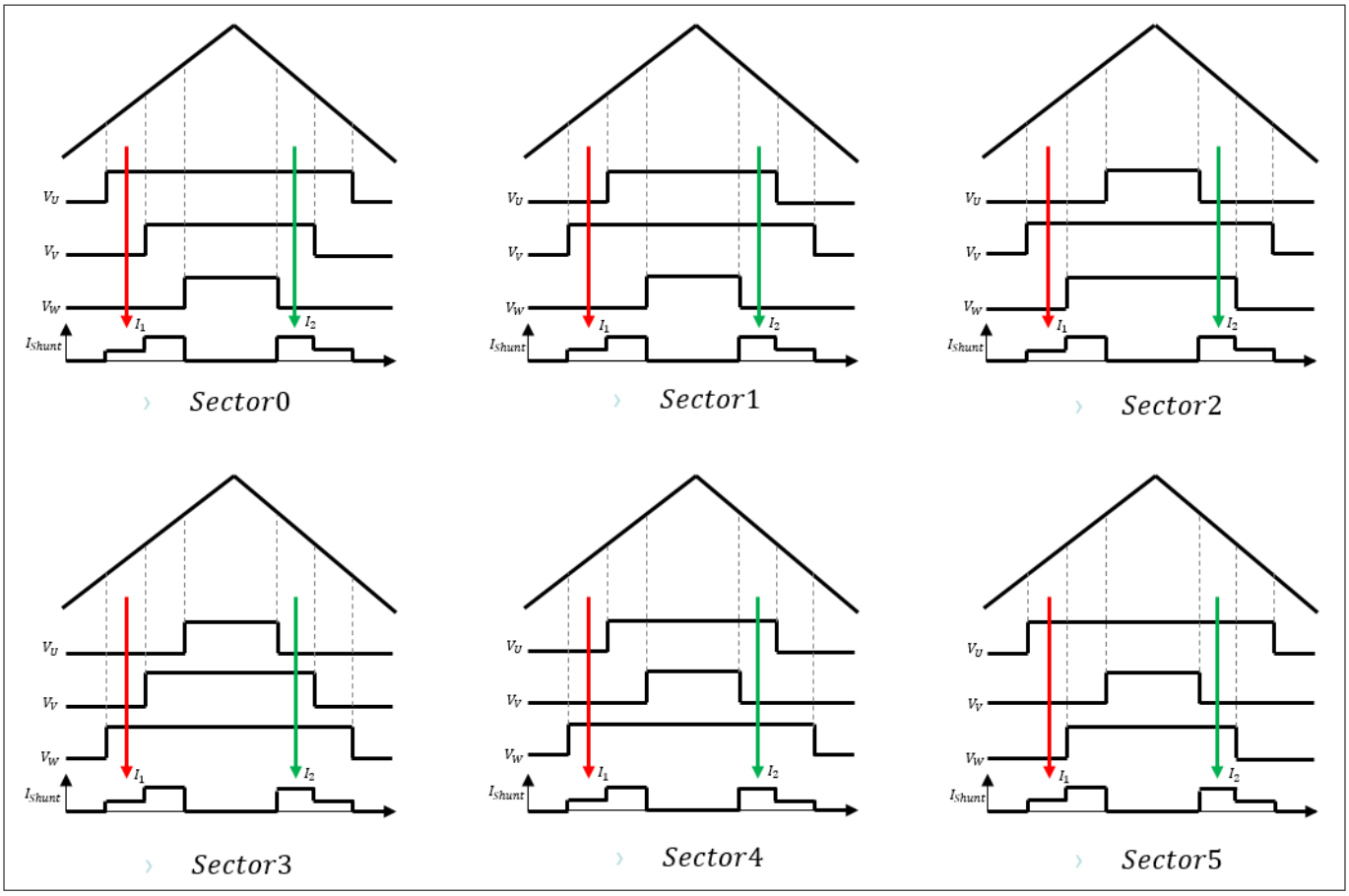

Figure 26 PWM synchronize sampling point each Sector

As you can observe in ***Figure 26***, these currents are sampled at two different times in the PWM cycle enabling measurement of different currents. They take place approximately halfway between the modulation of two phases which ensures the shunt current has stabilized. ***Figure 27*** shows this timing is achieved by utilizing Timer13 for this delay.

4 Software Block Diagram

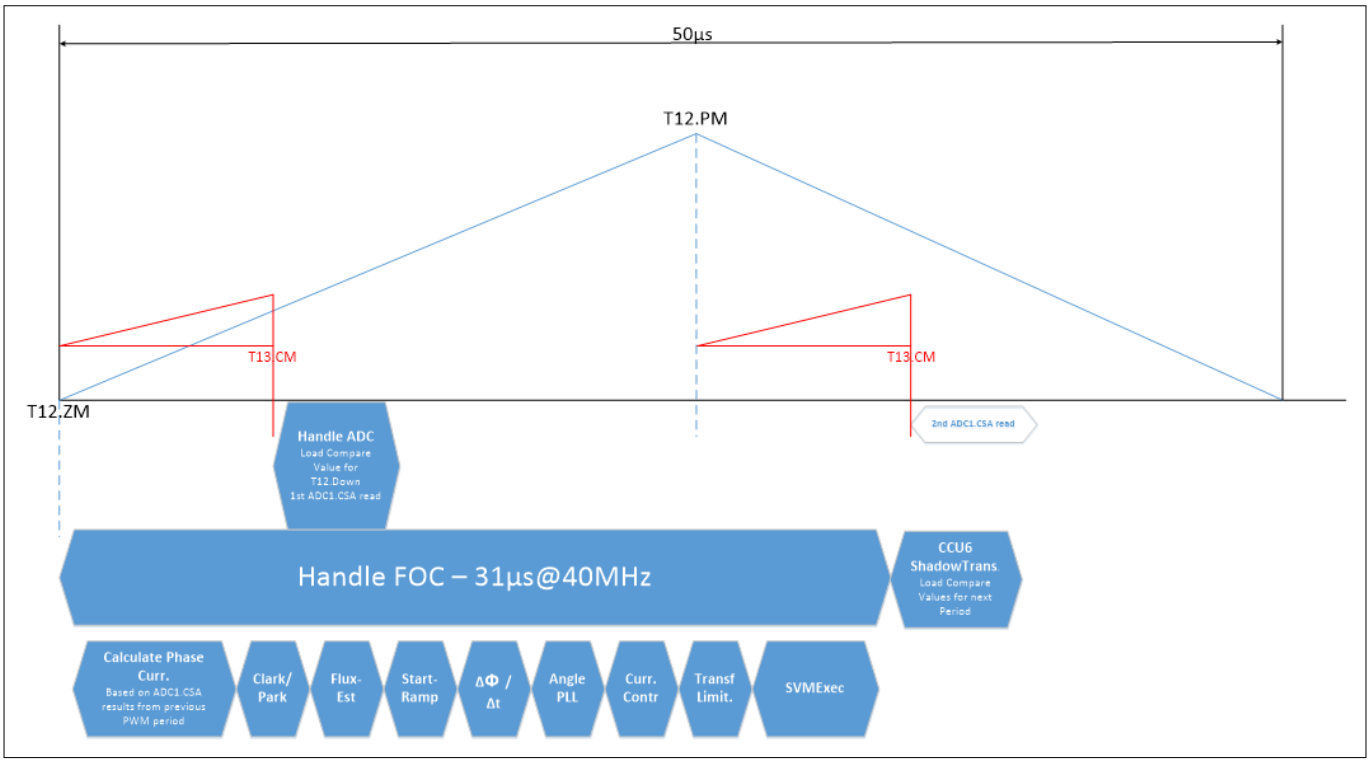

Figure 27 Current measurement and FOC calculation

Let's analyse ***Figure 26*** in more detail. For example, the first sampling in Sector0 measures the contribution of the only U phase current wether the second sampling measures the contribution of both U and V phase currents. Therefore, the current of U phase becomes I_1 and the current of V phase becomes $I_2 - I_1$. The current of W phase is calculated by $-I_2$ according to $I_U + I_V + I_W = 0$. This analysis can be performed for each invididual sector, and the results can be found in ***Table 3*** and ***Table 4***.

Table 3 Reconstruction mapping table

	I_V = PhasCurr.A	I_V = PhasCurr.B	I_W (not named in SW)
Sector0	I_1	I_2-I_1	-I_2
Sector1	I_2-I_1	I_1	-I_2
Sector2	-I_2	I_1	I_2-I_1
Sector3	-I_2	I_2-I_1	I_1
Sector4	I_2-I_1	-I_2	I_1
Sector5	I_1	-I_2	I_2-I_1

Table 4 The I_1 and I_2-I_1 applied offset

Variable	Formula	Symbol	Remark
R0mioffs	= AdcResult0 - Emo_Svm.CsaOffsetAdw;	I_1	Measurement within T_1
OffsmiR1	= Emo_Svm.CsaOffsetAdw - AdcResult1;	-I_2	Calculated
R1miR0	= AdcResult1 - AdcResult0;	I_2-I_1	Measurement within T_2

The variable definitions used by Infineon may seem arbitrary, they have constant properties over the PWM cycle, which explain their usage:

- "R0mioffs" is a stable positive current
- "OffsmiR1" is negative
- "R1miR0" is close to zero

as seen in ***Figure 28***.

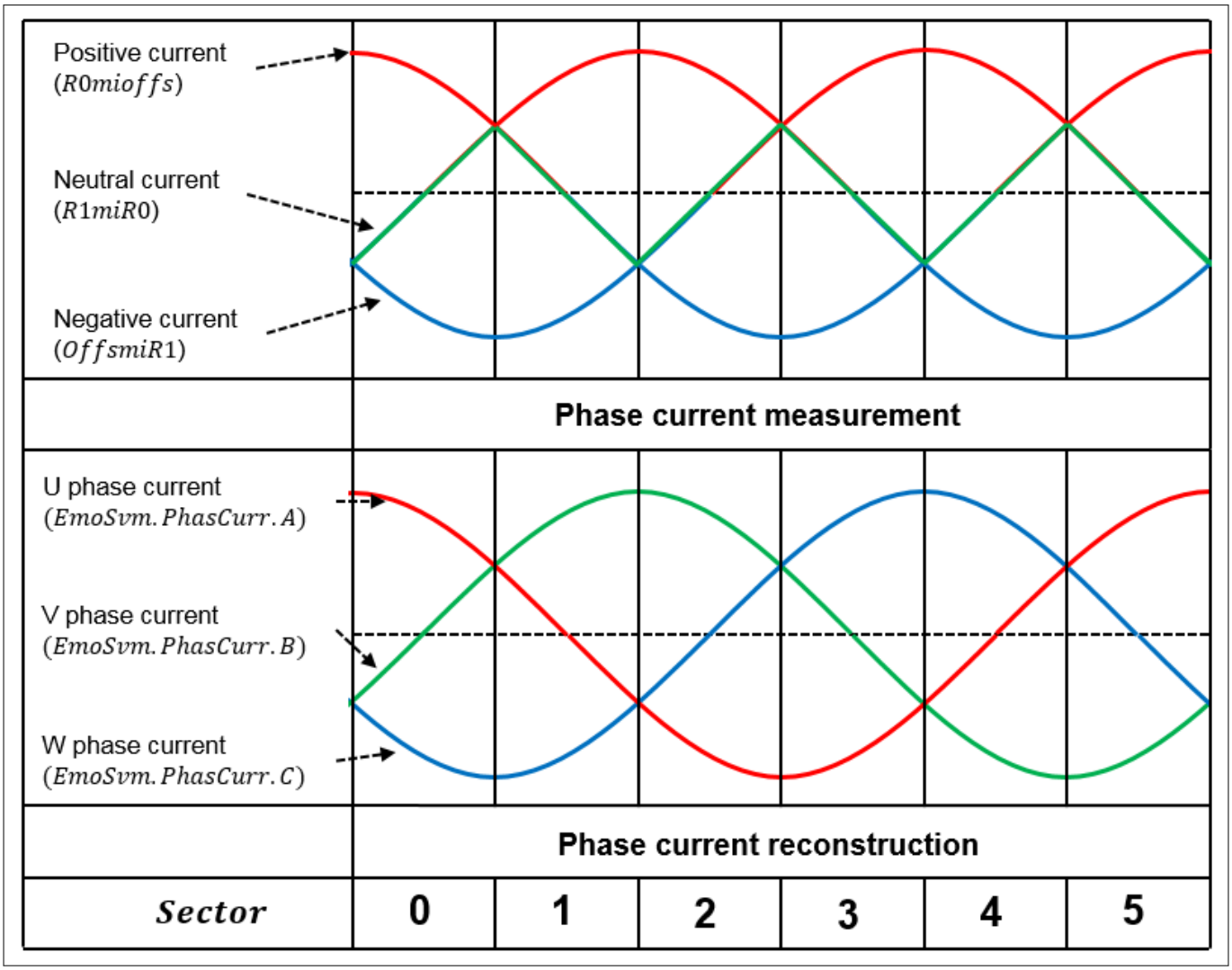

Figure 28 Phase current reconstruction

Once this mechanism is understood, the reconstruction process can be seen as the simple selection of the correct variable during each sector. For example, in order to reconstruct the U phase current, the positive current in sector 0, the neutral current in sector 1, the negative current in sector 2 and 3, the netural current in sector 4, the positive current in sector 5 are necessary.

4.2 Clarke Transform

As seen in the theory, the Clarke Transform converts the phase current stationary three-phase coordinate system into a two-phase stationary coordinate system (α, β), simplifying the control. It is essentially a projection into a Cartesian two-axis reference system. The factor 2/3 (marked in red) is required to keep the amplitude of the space vector in Cartesian coordinates at the same value as the amplitude of the original phase value.

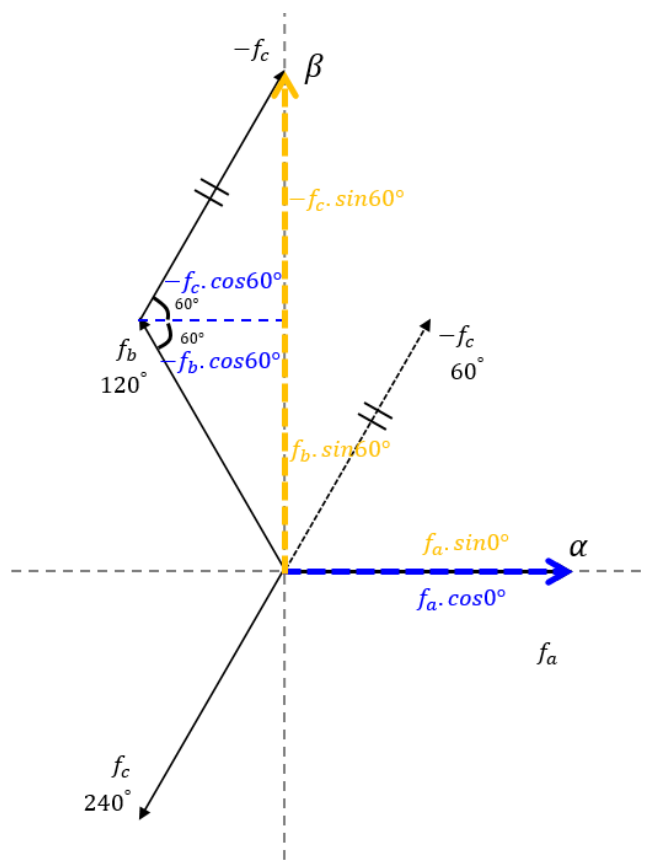

$$\alpha = f_a . cos0° - f_b . cos60° - f_c . cos60°$$

$$\alpha' = f_a - f_b\frac{1}{2} - f_c\frac{1}{2} = f_a - \frac{1}{2}(f_b + f_c) = f_a - \frac{1}{2}(-f_a)$$

$$\rightarrow \alpha = \frac{3}{2}f_a * \frac{2}{3} = f_a$$

$$\beta = f_a . sin0° + f_b . sin60° - f_c . sin60°$$

$$\beta' = f_b\frac{\sqrt{3}}{2} - f_c\frac{\sqrt{3}}{2} = \frac{\sqrt{3}}{2}(f_b - f_c)$$

$$\rightarrow \beta = \frac{\sqrt{3}}{2}(f_b - f_c) * \frac{2}{3} = \frac{1}{\sqrt{3}}(f_b - f_c)$$

Finally equation:

$$\alpha = f_a$$

$$\beta = \frac{1}{\sqrt{3}}(2f_b - f_a)$$

Equation 26 Clarke transform fomula

In the software, this responsability is handled by the Mat_Clarke function. ***Figure 29*** visually shows the result of simulating this function, which transforms a three-phase coordinate system into a two-phase coordinate system.

Input: 3phase current	Output: α, β
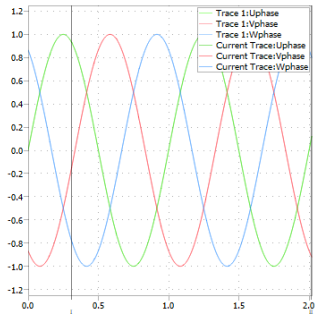	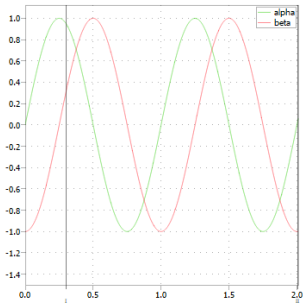

Figure 29 Clarke transform in PLECS

4.3 Park Transform

As stated in the theory, the Park Transform converts a two-variable fixed coordinate system to a two-variable rotating coordinate system. This means it transforms time-variant (AC) into time-invariant (DC) variables, simplifying control. The angle between the fixed and the rotating systems is the angle of the rotor θ.

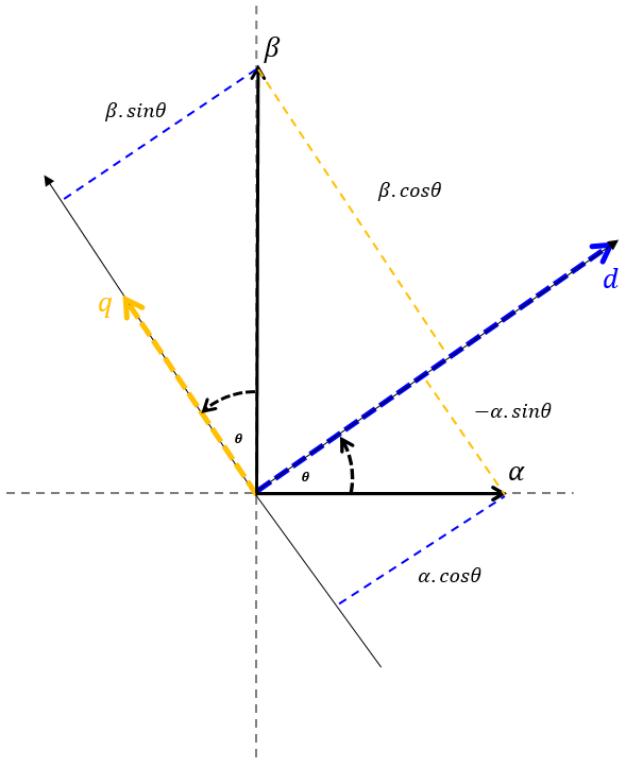

$$d = \alpha \,.\, cos\theta + \beta \,.\, sin\theta$$
$$q = -\alpha \,.\, sin\theta + \beta \,.\, cos\theta$$

Equation 27 Park transform formula

In the software, this responsability is handled by the Mat_Park function. ***Figure 30*** visually shows the result of simulating this function, which transforms a fixed coordinate system to the rotating coordinate system.

Input: α, β	Output: d, q
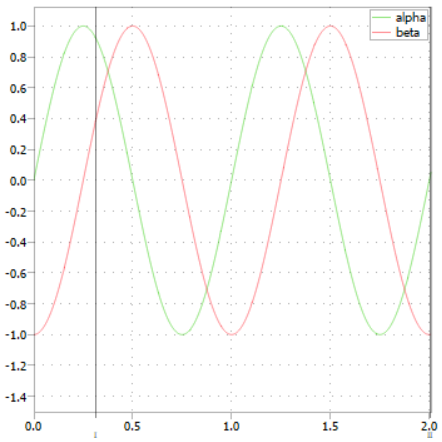	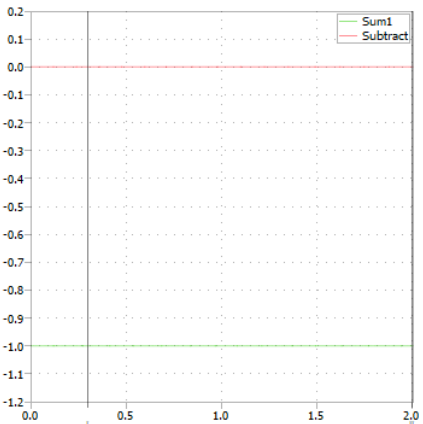

Figure 30 Park transform in PLECS

4.4 Polar to Cartesian Transform

The flux estimator in the Infineon example software requires variables in Cartesian coordinates. This is a standard mathematical transformation and its explanation is beyond the scope of this document.

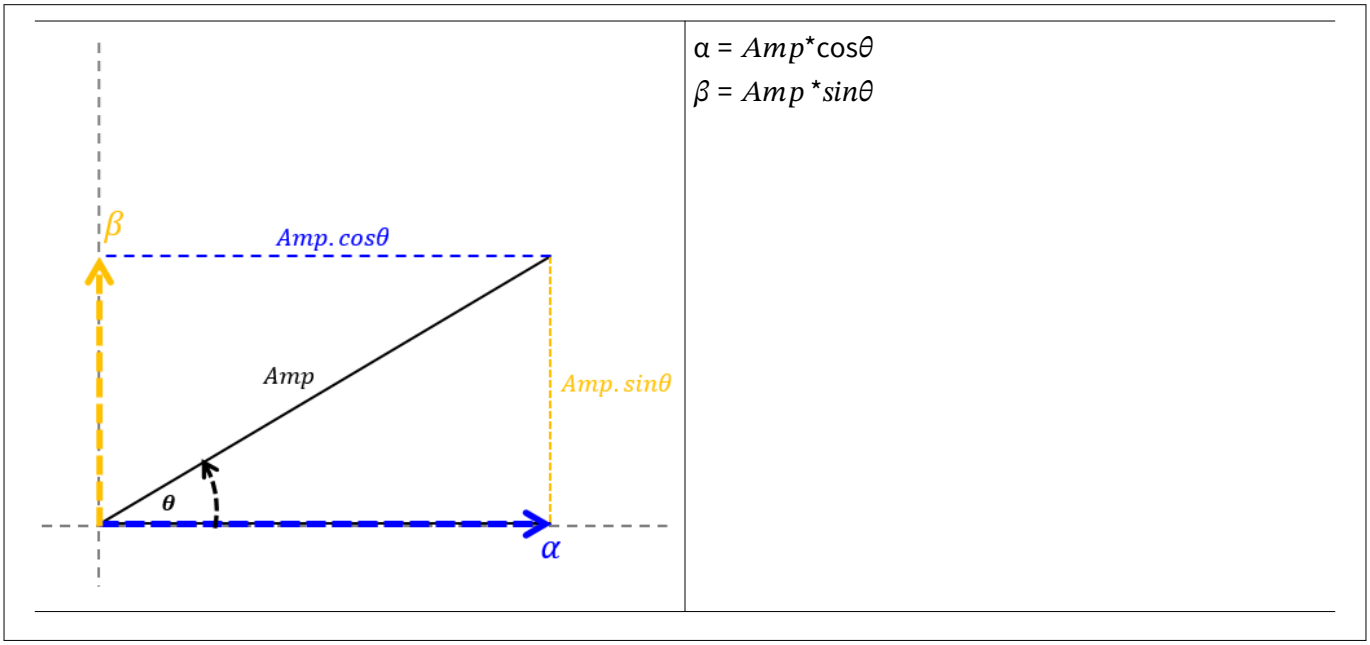

Equation 28 Cartesian transform formula

In the software, this responsability is handled by the Mat_PolarKartesisch function. ***Figure 31*** visually shows the result of simulating this function, which transforms polar to Cartesian coordinates.

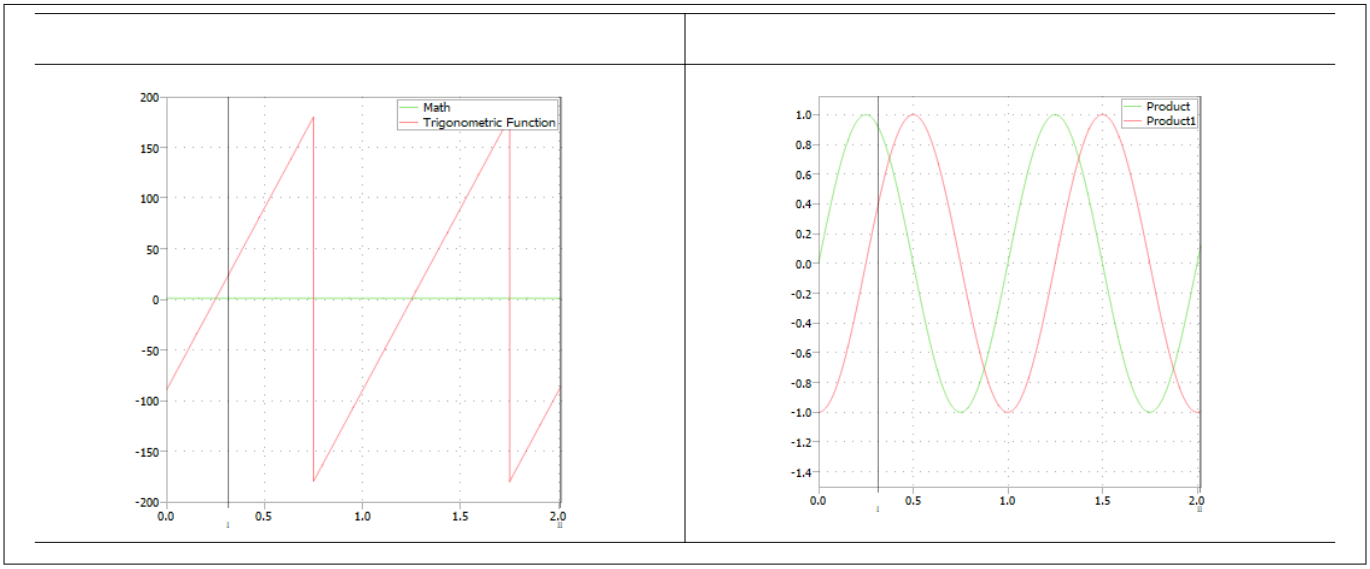

Figure 31 Cartesian transform in PLECS

4.5 Flux Estimator

As explained in the theory, in order to estimate the position of the rotor, the BEMF of the motor is calculated by the flux estimator. The flux estimator is based on the RL motor circuit equation seen in ***Equation 29***.

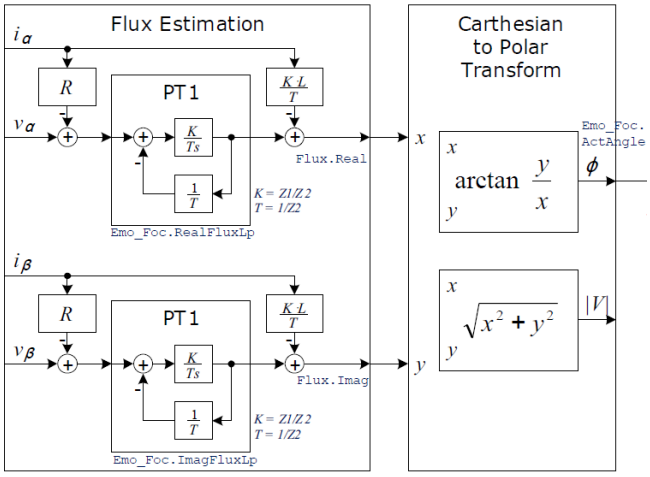

Estimating the flux linkage for α axis:

$$V_{s\alpha} = R_s \,.\, i_{s\alpha} + L\frac{di_{s\alpha}}{dt} + \frac{d\Psi_{s\alpha}}{dt}$$

$$\Psi_{s\alpha} = \int (V_{s\alpha} - R_s \,.\, i_{s\alpha})dt - L_s \,.\, i_{s\alpha}$$

$$Flux \,.\, Real$$

Estimating the flux linkage for β axis:

$$V_{s\beta} = R_s \,.\, i_{s\beta} + L\frac{di_{s\beta}}{dt} + \frac{d\Psi_{s\beta}}{dt}$$

$$\Psi_{s\beta} = \int (V_{s\beta} - R_s \,.\, i_{s\beta})dt - L_s \,.\, i_{s\beta}$$

$$Flux \,.\, Imag$$

Stator coordinates: Real-Imaginary to Module-Phase conversion equations:

$$EmoFoc \,.\, FluxAngle = \tan^{-1}\frac{Flux \,.\, Imag}{Flux \,.\, Real}$$

$$FluxAmp = \sqrt{Flux \,.\, Real^2 + Flux \,.\, Imag^2}$$

Equation 29 Flux Estimator formula

In the Infineon example software the current values are the estimated currents in the stator coordinate system (αβ) and the motor parameters are configured by the user during programming.

In the software, this responsability is handled by the emo_lEstFlux function. ***Figure 32*** visually shows the result of simulating this function, which estimates the angle.

Input: v_α, v_β, i_α, i_β

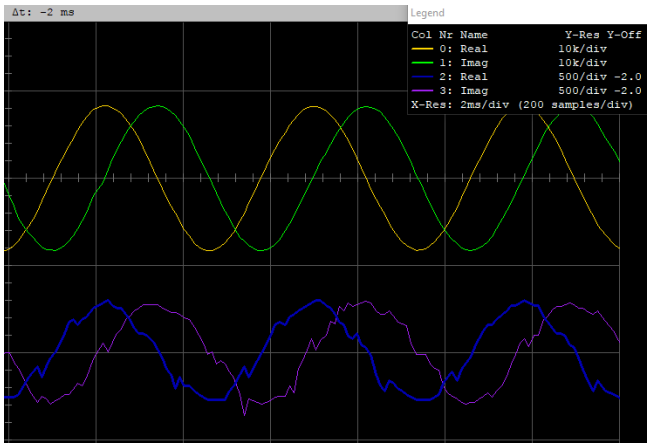

Output: Angle

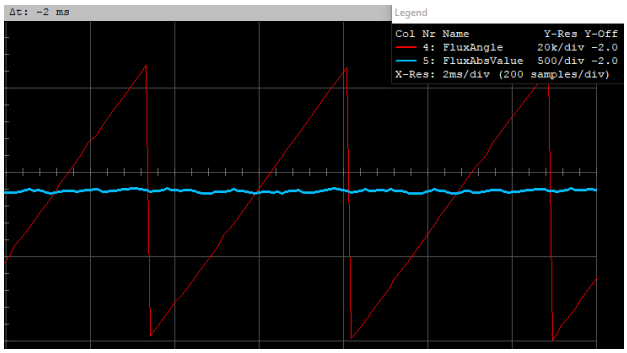

Figure 32 Flux Estimator in J-Scope

4.6 Angle PLL Observer

The main purpose of the PLL is to stabilize the angle position during the next PWM cycle based on measured angle position, last known angle position and estimated speed. As shown in ***Equation 30***, the PLL is implemented via a regulation loop, which filters the angle output.

The P-Controller of the PLL should be dimensioned as follows: fast enough to follow the maximum expected system dynamics, but slow enough to filter out angle errors caused by high frequency disturbances. Getting an optimal solution to this problem usually requires testing on the complete system.

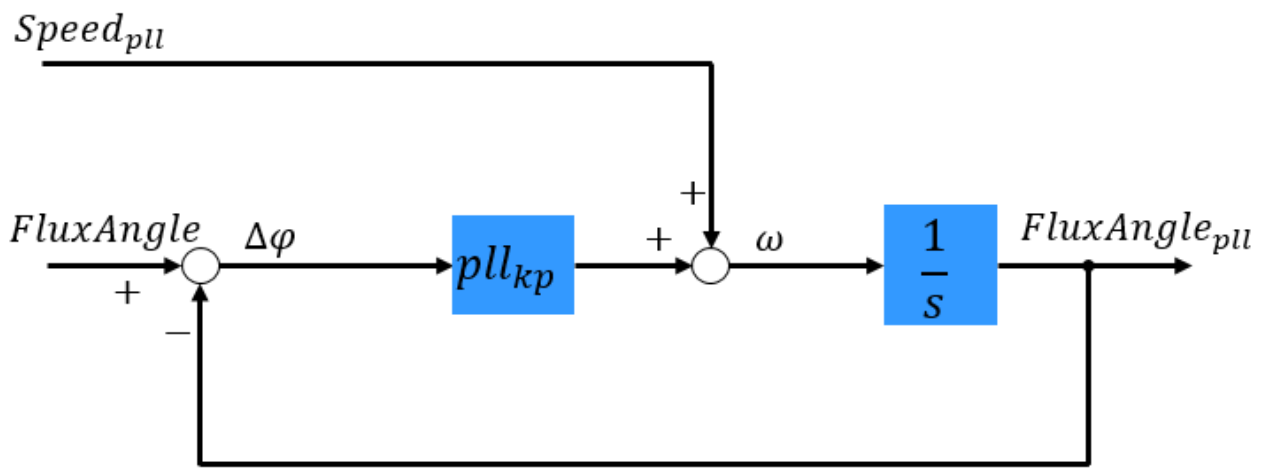

$$FluxAngle_{pll} = Speed_{pll} + pll_{kp}\int\varphi(t)dt$$

$FluxAngle$: *estimated angle*

$\Delta\varphi$: *error of angle*

ω: *estimated angular velocity*

$FluxAngle_{pll}$: *output angle*

Equation 30 Angle PLL Observer

In the software, this responsability is handled by the Emo_FluxAnglePll function. ***Figure 33*** visually shows the result of simulating this function, which produces a smoother angle estimation (in green).

Input: FluxAngle, $Speed_{pll}$	Output: $FluxAngle_{pll}$

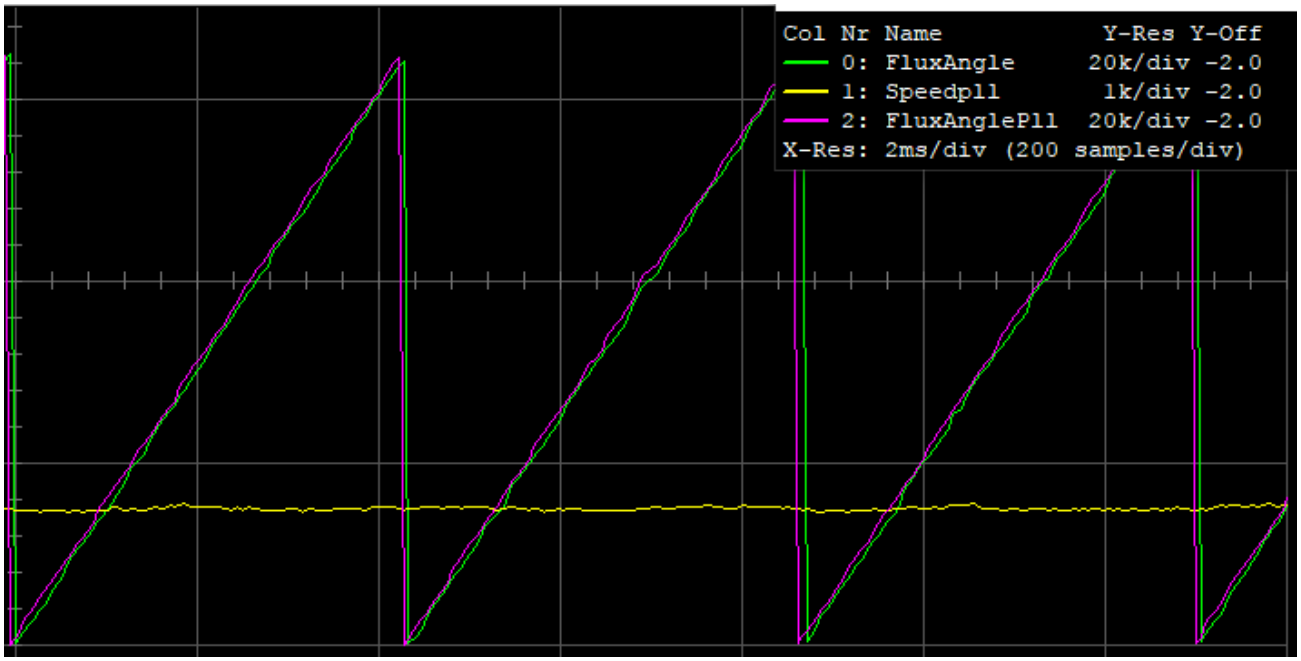

Figure 33 PLL controller in J-Scope

4.7 PI Controller

Infineon's example software includes two PI Controllers, which regulate the torque and speed in the motor drive system. PI controllers combine the proportional controller and the integral controller to eliminate the steady state error of proportional controllers while obtaining their quick response characteristics.

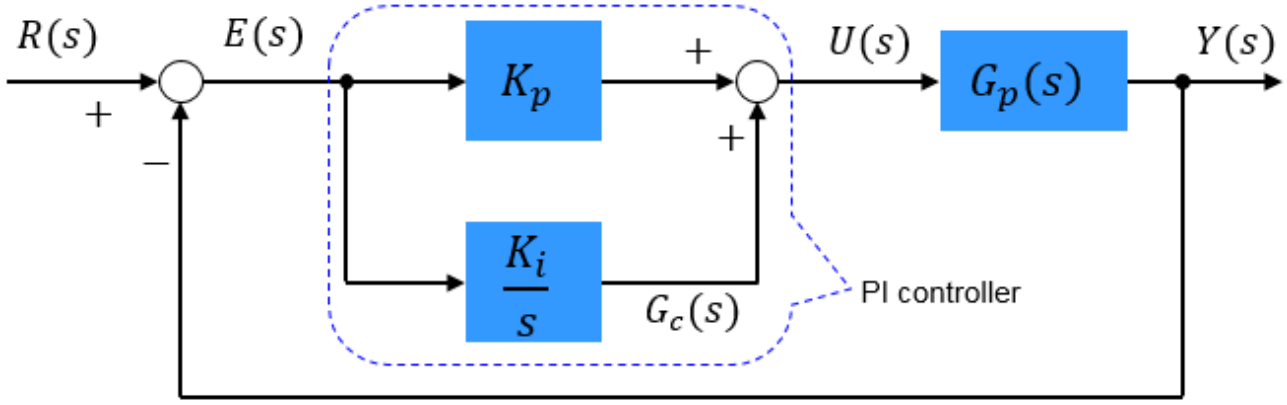

$Control\ input:\ U(t) = K_p e(t) + K_i \int e(t)dt$

$R(s): target\ value$
$E(s): error$
$U(s): control\ \ input$
$Y(s): control\ output$
$G_c(s): controller$
$G_p(s): system$

Equation 31 PI controller formula

In the software, this responsability is handled by the Mat_ExePi function. ***Figure 34*** compares the control input and output values for a PI controller.

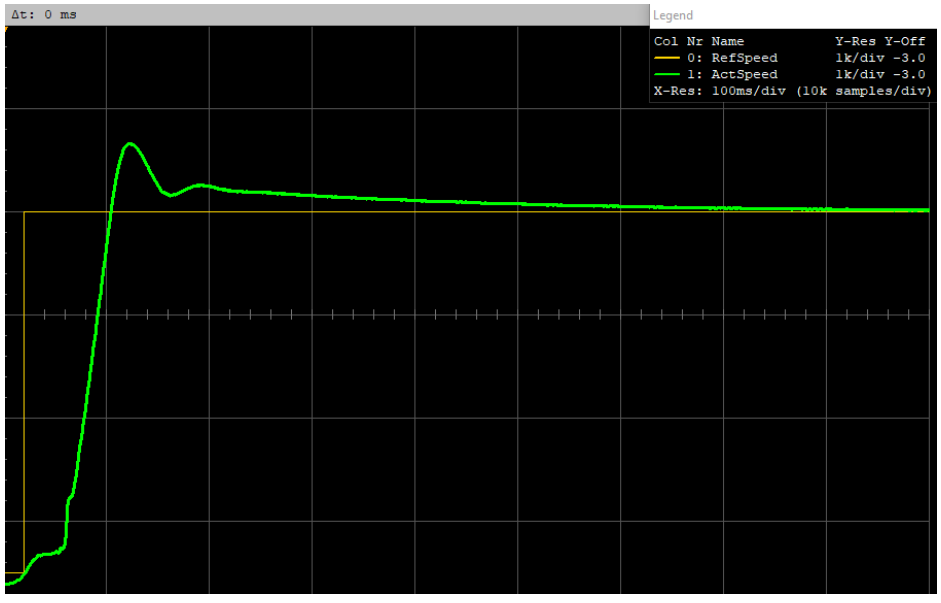

Figure 34 PI controller in time domain

4.8 Cartesian to Polar Transform

The SVM module in the Infineon example software requires variables in polar coordinates. This is a standard mathematical transformation and its explanation is beyond the scope of this document.

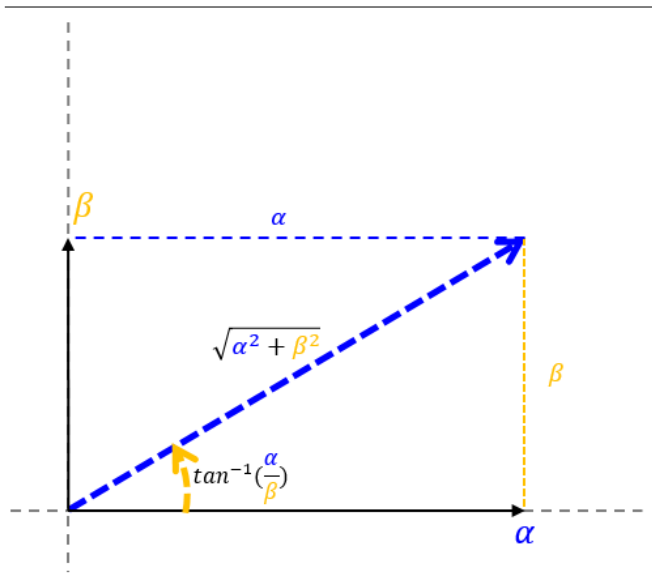

$$Amp = \sqrt{\alpha^2 + \beta^2}$$

$$\theta = tan^{-1}\left(\frac{\alpha}{\beta}\right)$$

Equation 32 Polar transform formula

In the software, this responsability is handled by the Mat_CalcAngleAmp function. ***Figure 35*** visually shows the result of simulating this function, which transforms Cartesian to polar coordinates.

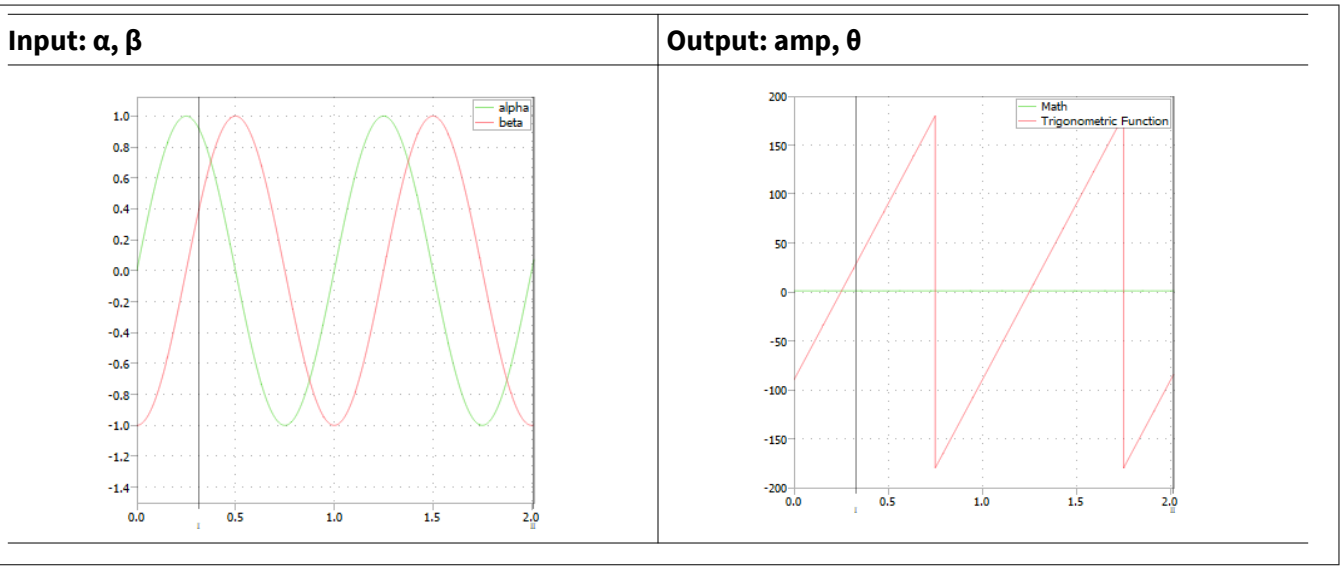

Figure 35 Polar transform in PLECS

4.9 SVM (Space Vector Modulation)

Space Vector Voltage Modulation (Space Vector PWM) is aimed to represent the reference vector V_{ref}, characterized by a certain amplitude and angle, as the superposition and scaling (simultaneous PWM modulation) of two active vectors in the space vector diagram.

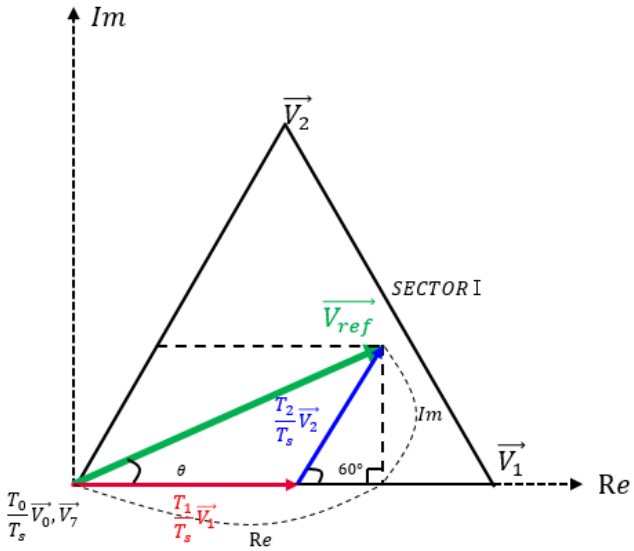

If the reference voltage vector is located in the region (0 ≤ θ ≤ 60 °), the following formula is established.

$$Re: \overrightarrow{V_{ref}} . cos\theta . T_s = T_1 . \overrightarrow{V_1} + T_2 . \overrightarrow{V_2} . cos6$$

$$\boldsymbol{Im: \overrightarrow{V_{ref}} . sin\theta . T_s = T_2 . \overrightarrow{V_2} . sin60°}$$

$$Re: \overrightarrow{V_{ref}} . cos\theta . T_s = T_1 . \frac{2}{3}V_{DC} + T_2 . \frac{1}{3}V_{DC}$$

$$Im: \overrightarrow{V_{ref}} . sin\theta . T_s = T_2 . \frac{1}{\sqrt{3}}V_{DC}$$

From this equation, the allowed time of the valid voltage vector and the zero voltage vectors is as follows.

$$T_1 = \frac{\sqrt{3} . \overrightarrow{V_{ref}} . T_S . sin\left(60° - \theta\right)}{V_{DC}}$$

$$T_2 = \frac{\sqrt{3} . \overrightarrow{V_{ref}} . sin\theta . T_S}{V_{DC}}$$

Finally equation:

$$T_1 = T_s . m_a . sin(60° - \theta)$$

$$T_2 = T_s . m_a . sin\theta$$

$$T_0 = T_s - (T_1 + T_2)$$

$$m_a = \frac{\sqrt{3} . \overrightarrow{V_{ref}}}{V_{DC}}$$

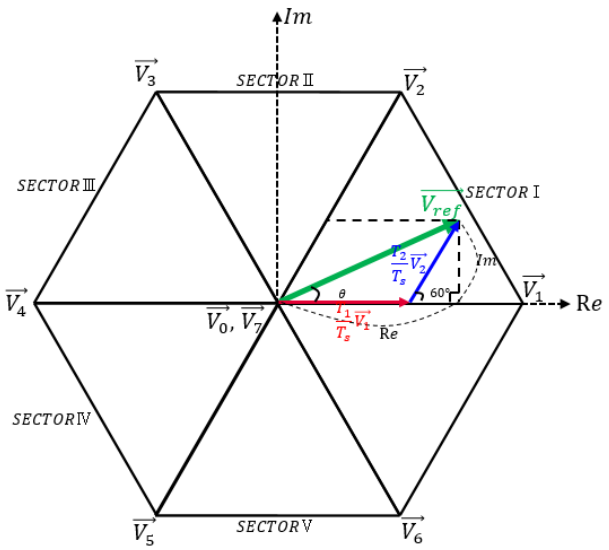

It is possible to obtain the valid voltage vector and the allowed time of the zero voltage vectors by performing the same calculation for the remaining sector Sector 2 to 6 regions.

Equation 33 SVM

In the software, this responsability is handled by the Emo_lExeSvm function. ***Figure 36*** visually shows the result of simulating this function, which transforms the valid voltage vector in polar coordinates into the modulation scheme for producing the MOSFET outputs.

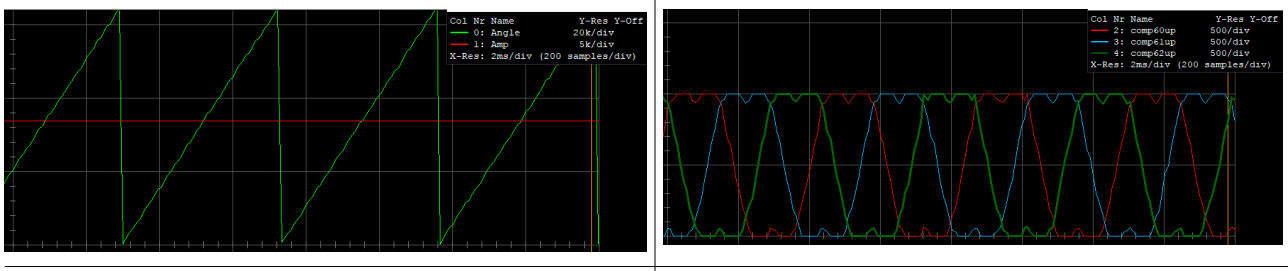

Figure 36 SVM in J Scope

5 Example Software

This section illustrates the practical aspects of using the Infineon example FOC software, such as which software programs are necessary, and the general layout of the software as a collection of files.

5.1 Tool chain

5.1.1 Compiler suite

This example uses KEIL compiler uVision5 (ARM Compiler, V5.22).

5.1.2 Debugger

This example uses KEIL compiler uVision5 as a software debugger and both Segger ***J-L ink LITE CortexM- 5V*** and ***XMC-LINK (KIT_XMC_LINK_SEGGER_V1)*** have been used as hardware debuggers.

5.1.3 SDK

5.1.4 ConfigWizard

This example uses Infineon's Config Wizard to set the initial register value for each peripheral block. This enables easy understanding of register functionality through a GUI as seen in ***Figure 37***. The selected values are then saved through the interface's file menu into a file with the structure xxx_defines.h which will be used by the SDK to setup the configuration registers of the compiled software.

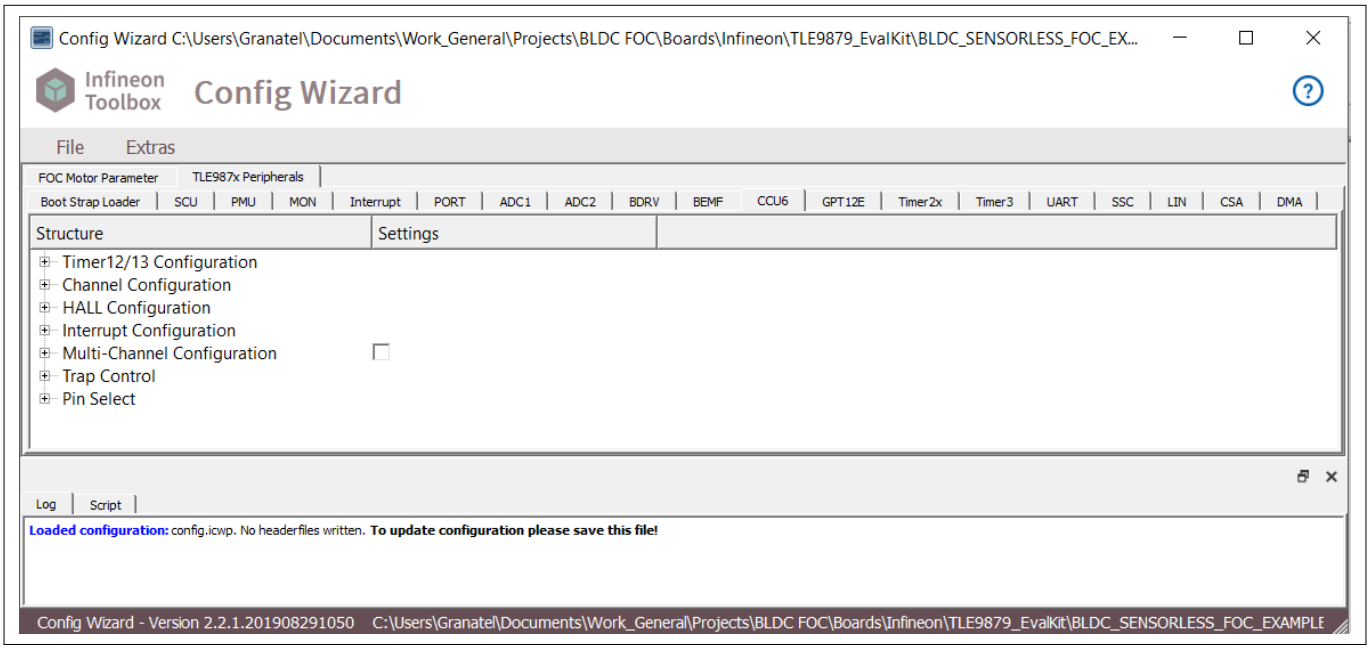

Figure 37 Config Wizard GUI

5.2 Example code & project layers

The Infineon example code can be downloaded free-of-charge through the uVision5 menu as seen in ***Figure 38***. Please open the Pack Installer from the uVision5 Build Toolbar. In the left menu, from the Devices tab, select “Infineon” and then in the “TLE987X Series” select the device you will be working with. In the right menu, from the “Examples” tab, you can find and copy the “BLDC Sensorless FOC” code.

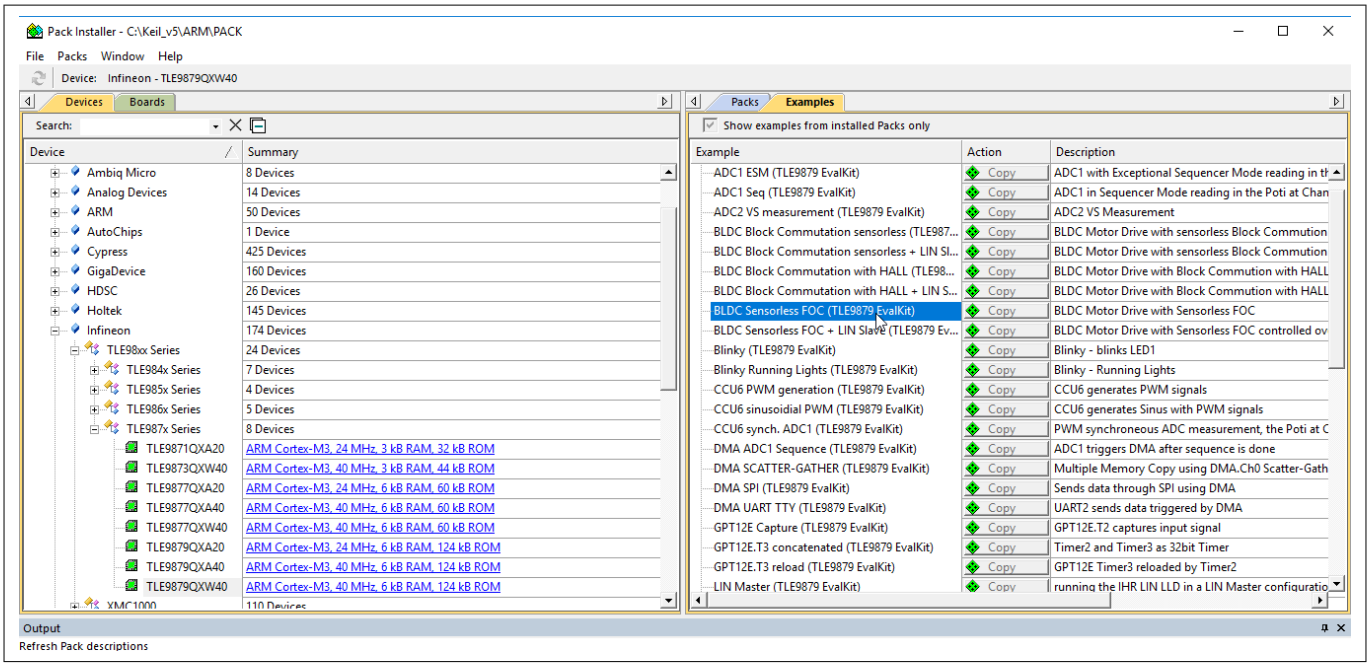

Figure 38 BLDC Sensorless FOC Example Location within the Keil uVision5 Pack Installer

The example software project consists of three main layers called “app”, “emo” and “Devices” as described in ***Figure 39***.

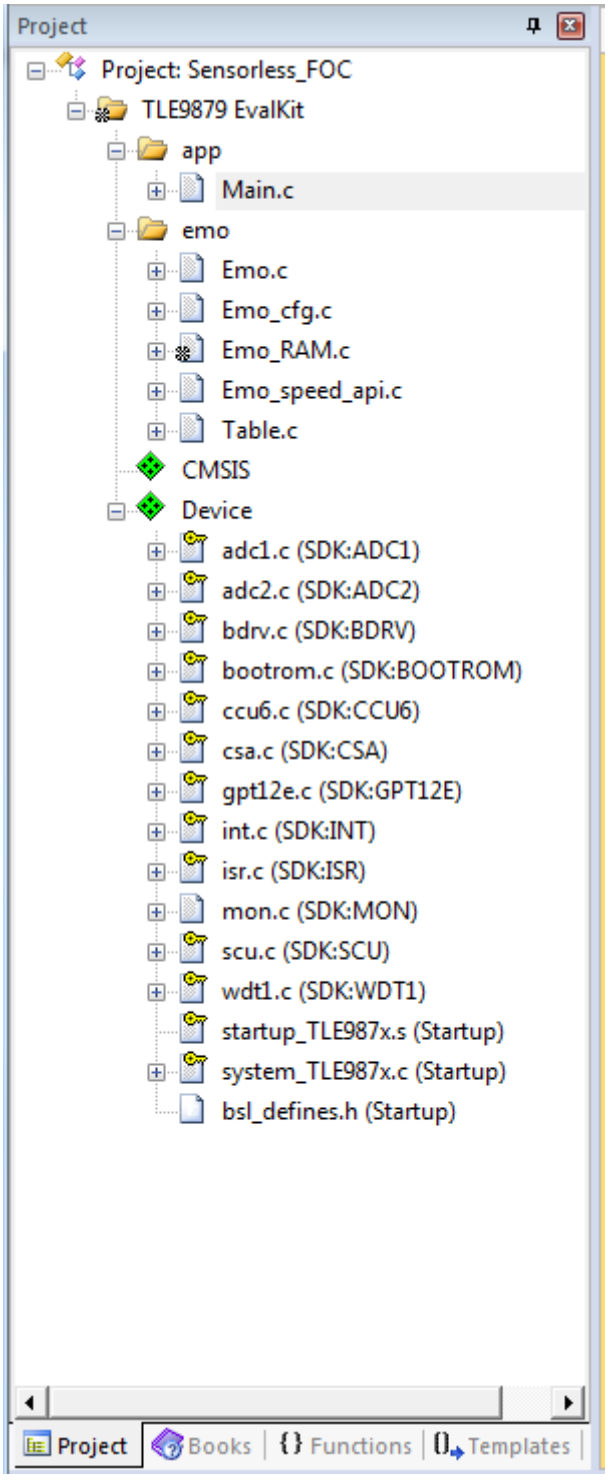

Figure 39 Software Project Layers

5.2.1 “App”

The “app” layer is left intentionally limited in functionality for users to implement further features in this layer depending on their application’s requirements. Typical examples include communication and monitoring software.

File	Main functionality
main.c	Core of the program, motor start/stop control

5.2.2 “Emo”

The files found in the “emo” layer are related to the motor control. These files may also be edited by the user in order to modify motor behavior or monitor particular parts of the software.

File	Main functionality
Emo.c	FOC initialization example, FOC programming in memory
Emo_cfg.c	Configuration values from FOC Motor Parameter tab in ConfigWizard
Emo_RAM.c	FOC programming in RAM
Emo_speed_api.c	Speed control function
Table.c	Tables for mathemicatical operations such as: Sin, Sin60, Cos, ArcTan

5.2.3 “Device”

Device related files are automatically installed both on the FOC example code and more generally, on all software projects generated for the TLE987X and coded in KEIL uVision 5. These files contain initialization and control functions provided in order to access the capabilities of each hardware module in the chip. If a user wants to change or optimize device files, it is highly recommended recommend to copy the device files from their original shared location into the project folder and update the files. To be able to edit the device files one must modify their Properties and uncheck the “read only” check box.

File	Main functionality
adc1.c / adc1.h	Defines, initialization functions and control functions for the ADC1
adc2.c / adc2.h	Defines, initialization functions and control functions for the ADC2
...	Defines, initialization functions and control functions for other hardware modules

5.3 FOC parameter configuration

The example software requires a minimal amount of FOC parameter configuration in order to run most motors. The FOC parameter configuration can be performed via the Configwizard GUI, in the FOC Motor Parameter tab. This secton provides a simple explanation of the parameters in that tab.

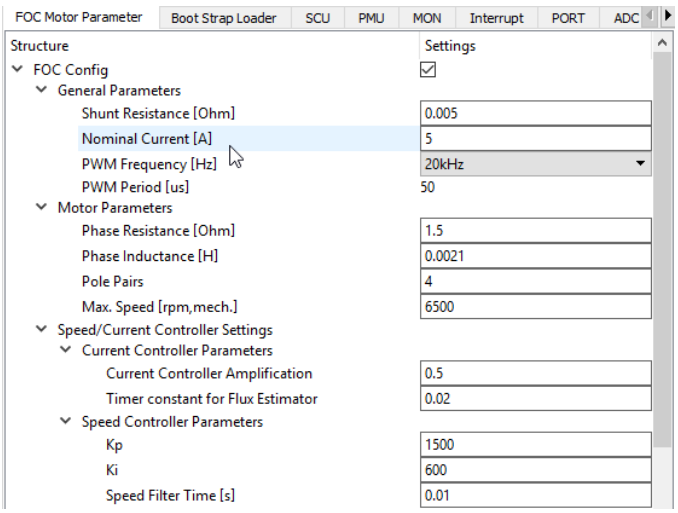

Shunt Resist.[Ohm]: 5mΩ in eval kit

If other board: RShunt≤ 120mV/INOM

Nominal Current [A]: Max. expected peak phase current

PWM Frequency [Hz]: 10~25kHz

PWM Period calculated depending on frequency

Phase Resistance [Ohm] & Phase Inductance [H]: As measured, converted from star (/2) or delta (*1.5)

Pole Pairs & Max. Speed [rpm.mech.]: Determined by motor

Current Controller Amplification: Scales current control loop speed between 0.01 (slow) and 1 (fast)

Timer constant for Flux Estimator: K_B for flux estimator

Kp: Affects regulator speed

Ki: Affects regulator error

Speed Filter Time [s]: Low pass filter for speed, between 0.01 (slow) and 1 (fast)

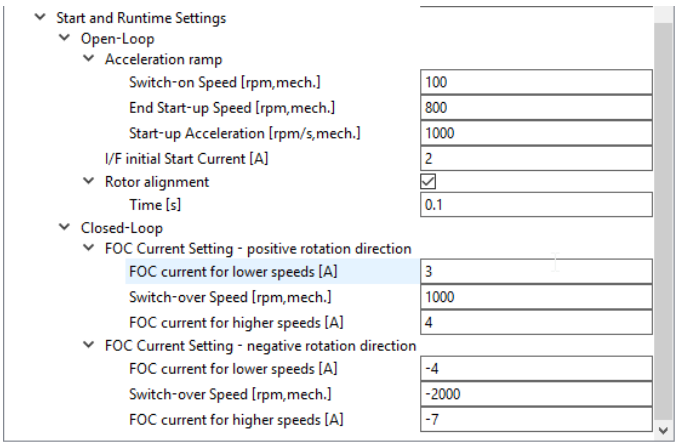

Switch-on Speed [rpm.mech.]: Beginning open loop speed

End Start-up Speed [rpm,mech.]: Speed at end of open loop

Start-up Acceleration [rpm/s,mech.]: Acceleration during open loop

I/F initial Start Current [A]: Current limit during open loop – see ***Figure 40***

Rotor alignment time [s]: Time to place the rotor in a known position before running – see ***Figure 40***

Closed loop settings:

Direction dependent like many applications

FOC current for lower speeds [A]

Switch-over Speed [rpm,mech.]

FOC current for higher speeds [A]

Current limits for low and high speeds during closed loop operation, and limit between the two - Figure 51

The setting of these parameters strongly depends on the respective motor characteristic and application requirements. Infineon is happy to help customers find the correct parameters for their application.

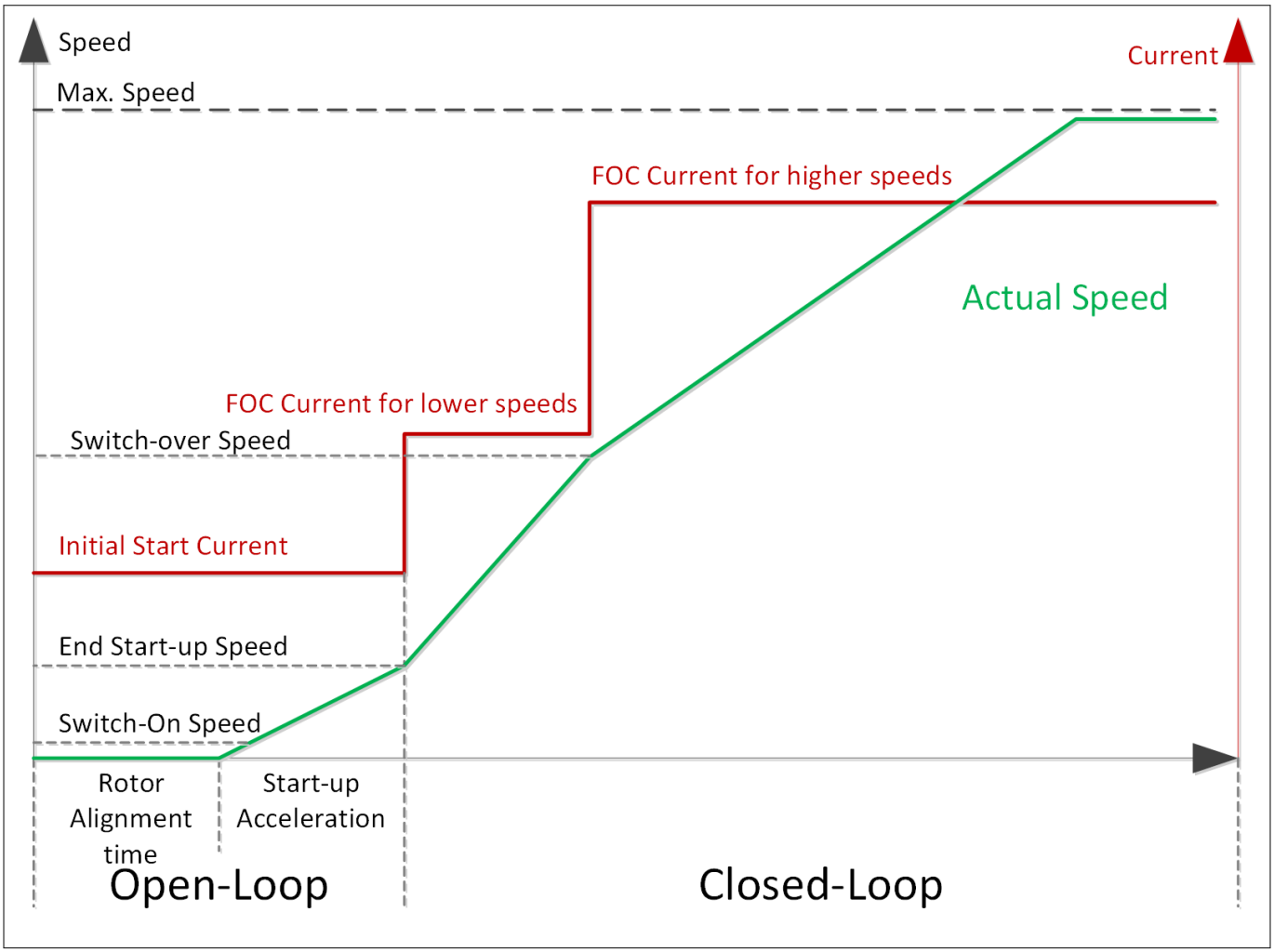

Figure 40 Startup Behaviour

In case a customer would like to tune the FOC Parameter control, the following has been proven by Infineon's experience to be a useful algorithm:

1. Set Shunt Resistor, Norminal Current and PWM Frequency
2. Find and set motor parameters from motor data sheet
3. Set Kp, Ki and speed time in speed controller
4. Set Acceration ramp control (depending on motor and load condition)
5. Set rotor alignment time (set long time first, then reduce progressively)
6. Set Min/Max current in closed loop control and switch over speed
7. Repeat Step 3) to Step 6) to find the best fitting parameters.

5.4 How to Start

5.4.1 Test conditions

5.4.1.1 Test environment

The test environment consists of a TLE9879 evaluation kit, a J-Link Ultra+, a power supply and example code + example code “BLDC_SENSORLESS_FOC_EXAMPLE_TLE987X” for Sensorless BLDC application.

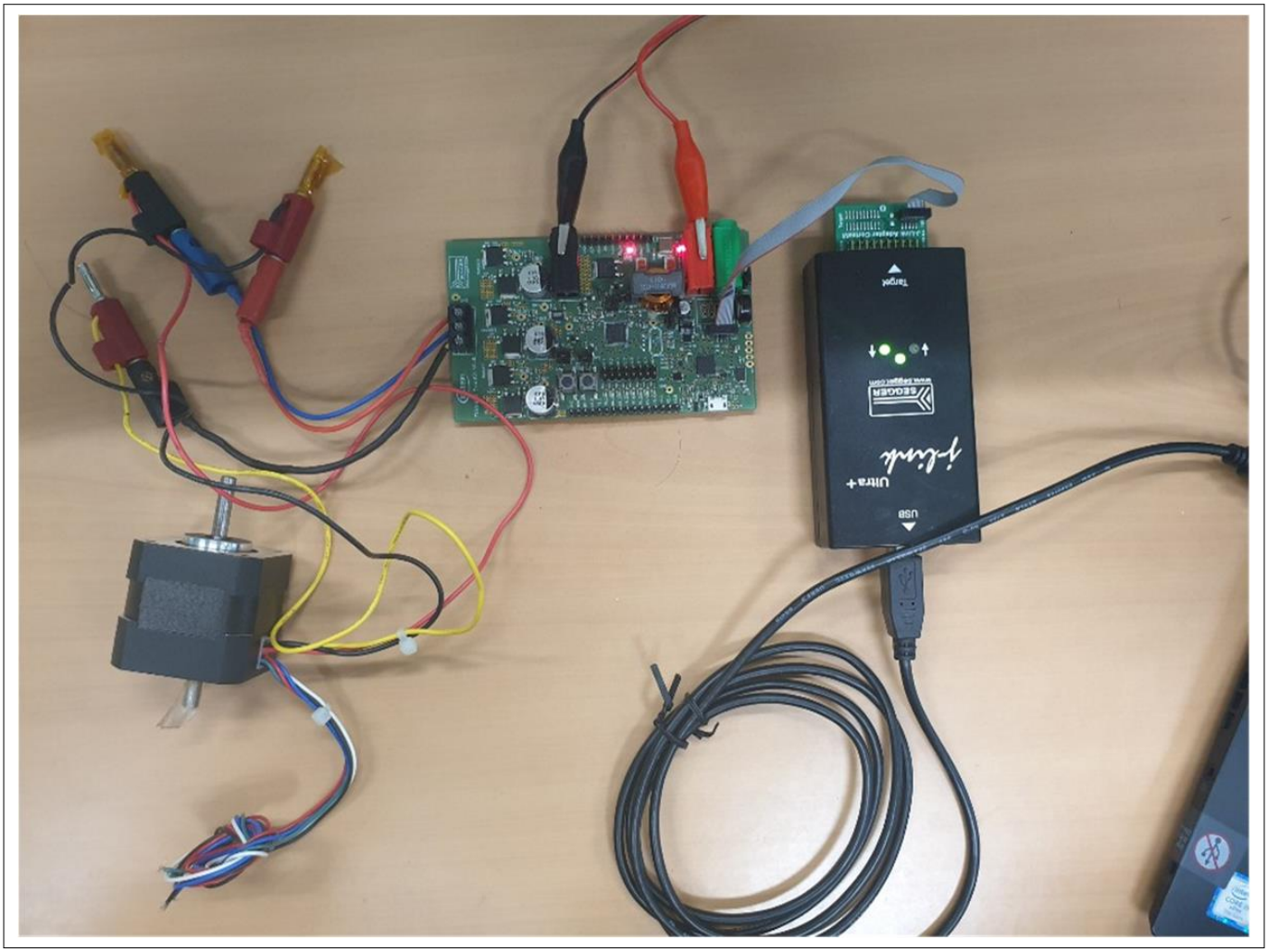

Figure 41 Test environment

5.4.1.2 ConfigWizard parameters

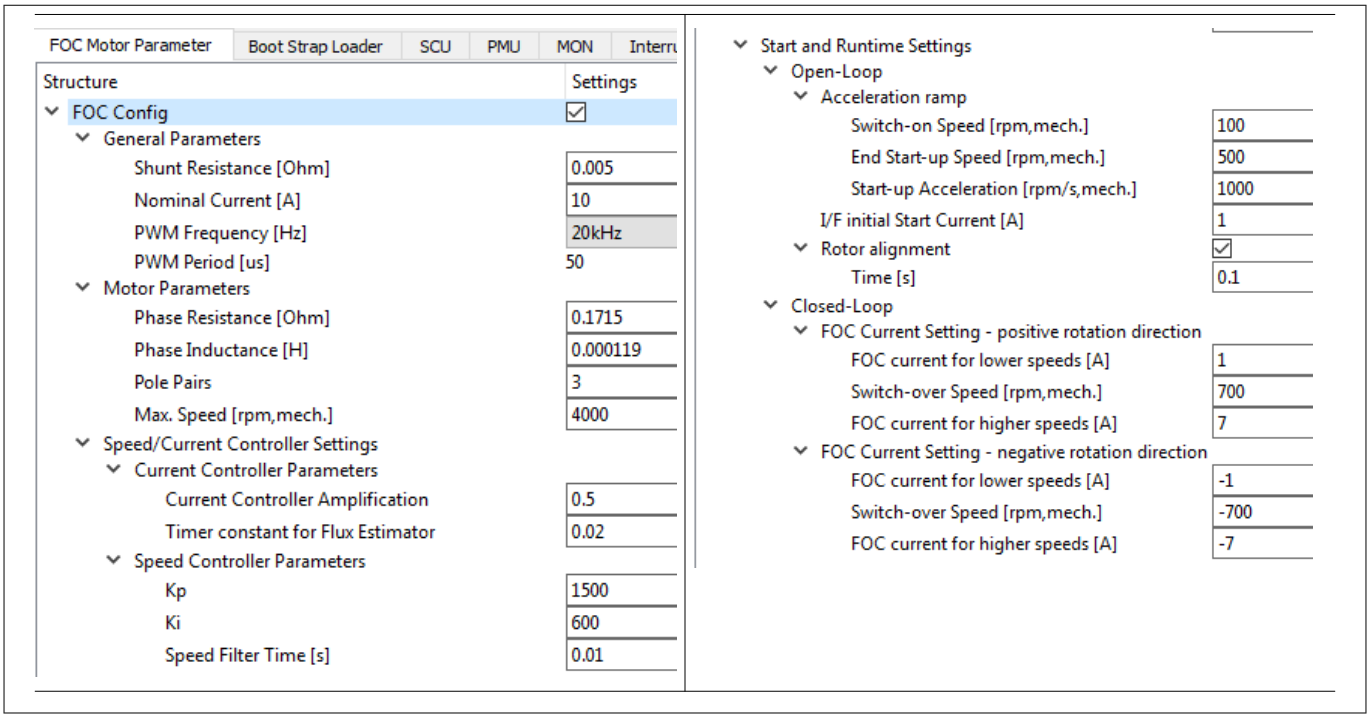

Figure 42 Test case configwizard parameters

5.4.1.3 Startup test

Figure 43 shows how the motor operates after pressing the motor operation button MON1 to reach the targetted RPM of 4000 RPM. After switching from EMO_MOTOR_STATE_STOP to EMO_MOTOR_STATE_START, the motor increases its speed and then switches to EMO_MOTOR_STATE_RUN.

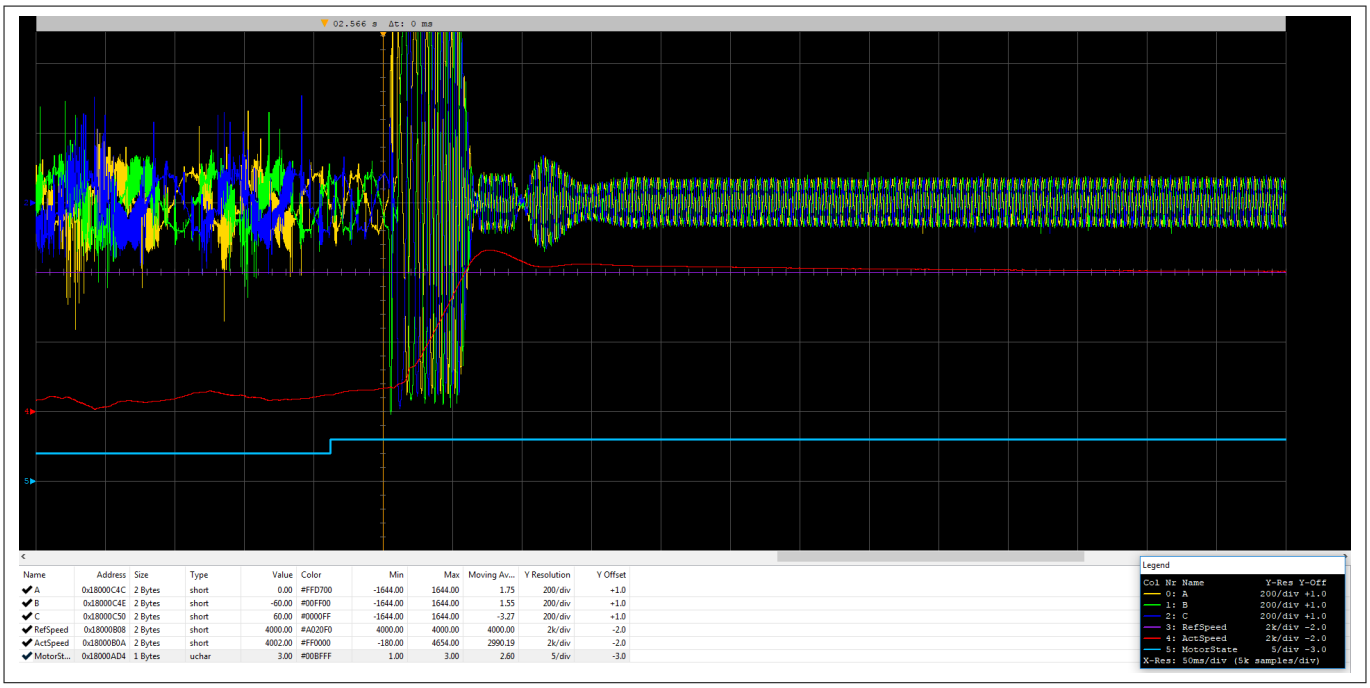

Figure 43 Startup test in J-Scope

5.4.1.4 Perform whole Software Block

Figure 44 shows how software blocks behave, sequentially. The variables pictured are, respectively, the phase current measurement, Clark Transform, Park Transform, Flux Estimator,Polar Transform, and SVM output to the MOSFETs.

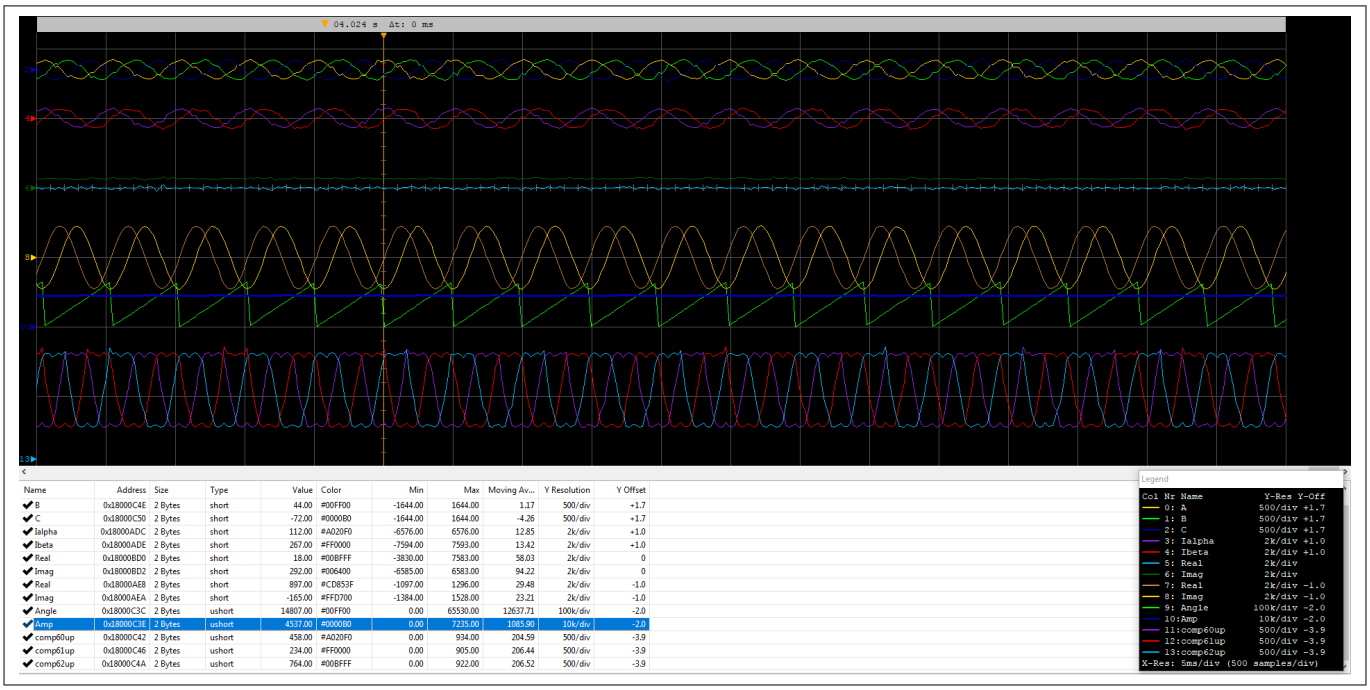

Figure 44 Perform while Software Block in J-Scope

6 Conclusions

This application note shows how the user can develop the Field Oriented Control scheme in a straightforward Hardware and Software implementation with the TLE9879. This is indeed possible thanks to the versatility of the integrated ADC, Bridge Driver, CCU6 and Current Sense Amplifier, which accommodate the timing and synchronization needed by the scheme complexity. These blocks constitute the bone structure of the FOC feedback loop, completed by the motor control software implementation which eventually allows to perform:

- phase current measurements
- trigonometric transforms
- flux and angle estimation
- PI Controller
- Space Vector Modulation (SVM)

The capabilities of the TLE9879 are demonstrated by the "BLDC Sensorless FOC" example code downloadable through the SDK and made easy to use thanks to the ConfigWizard and its "FOC Motor Parameter" extension panel. With this example the user can setup, personalize and optimize the FOC scheme to its own use cases, making the "BLDC Sensorless FOC" example code a useful starting point for developing typical applications.

7 References

[1] Application note - AP0807120_DriveMonitor, Infineon Technologies AG ***https://www.infineon.com/dgdl/ap0807120_DriveMonitor.pdf?fileId=db3a304316f66ee8011711879c203abc***

[2] Application note - AP08088, XC878CM DriveCard, Infineon Technologies AG ***https://www.infineon.com/dgdl/AP0808810_XC878DriveCard.pdf?fileId=db3a30431ed1d7b2011f645ccc54059d***

[3] [3] Application note - AP16179, XC2236N Drive Card Description, Infineon Technologies AG ***https://www.infineon.com/dgdl/ap1617910_DriveCard_XC2236N.pdf?fileId=db3a30432a14dd54012a235c4559017f***

[4] Application note - AP08059, Sensorless Field Oriented Control for PMSM Motors, Infineon Technologies AG ***https://www.infineon.com/dgdl/AP0805910_Sensorless_FOC.pdf?fileId=db3a3043134dde6001134e2c3cff002f***

[5] Application note - AP08090, Sensorless Field Oriented Control (FOC) on XC878, Infineon Technologies AG ***https://www.infineon.com/dgdl/ap0809010_Sensorless_FOC_XC878.pdf?fileId=db3a304320896aa20120d245735250c3***

[6] Application note - AP08090, XE166 Sensorless FOC, Infineon Technologies AG ***https://www.infineon.com/dgdl/ap1616510_XE166_Sensorless_FOC.pdf?fileId=db3a30432239cccd0122e49804bc3c38***

[7] Application note - AP16180, XC2000 Sensorless Field Oriented Control, Infineon Technologies AG ***https://www.infineon.com/dgdl/ap1618010_XC2000_Sensorless_FOC.pdf?fileId=db3a30432b16d655012b1a98fc182d9d***

[8] Data Sheet - TLE9879QXA40 Microcontroller with LIN and BLDC MOSFET Driver for Automotive Applications ***https://www.infineon.com/dgdl/Infineon-TLE9879QXA40-DS-v01_00-EN.pdf?fileId=5546d4625a888733015a89d10a283f20***

[9] User Manual - TLE9879 EvalKit V1.3 User Manual ***https://www.infineon.com/dgdl/Infineon-TLE9879_EvalKit-UserManual-v01_30-EN.pdf?fileId=5546d4626bfb5124016c0f44edaa201a***

[10] Motor Handbook, RWTH Aachen University and Infineon Technologies AG

Revision history

Document version	Date of release	Description of changes
V 1.0	2020-03-09	• Initial release

Trademarks

All referenced product or service names and trademarks are the property of their respective owners.

Edition 2020-03-09

Published by

Infineon Technologies AG

81726 Munich, Germany

Do you have a question about any aspect of this document?

Email: erratum@infineon.com

Document reference
IFX-oak1574952502462

IMPORTANT NOTICE

The information contained in this application note is given as a hint for the implementation of the product only and shall in no event be regarded as a description or warranty of a certain functionality, condition or quality of the product. Before implementation of the product, the recipient of this application note must verify any function and other technical information given herein in the real application. Infineon Technologies hereby disclaims any and all warranties and liabilities of any kind (including without limitation warranties of non-infringement of intellectual property rights of any third party) with respect to any and all information given in this application note.

The data contained in this document is exclusively intended for technically trained staff. It is the responsibility of customer's technical departments to evaluate the suitability of the product for the intended application and the completeness of the product information given in this document with respect to such application.

WARNINGS

Due to technical requirements products may contain dangerous substances. For information on the types in question please contact your nearest Infineon Technologies office.

Except as otherwise explicitly approved by Infineon Technologies in a written document signed by authorized representatives of Infineon Technologies, Infineon Technologies' products may not be used in any applications where a failure of the product or any consequences of the use thereof can reasonably be expected to result in personal injury